

**PROCESS WINDOWS CONSIDERING TWO CONFLICTING CRITERIA: THE
INJECTION MOLDING CASE**

by

Alicia Berenice Rodríguez Yáñez

A thesis submitted in partial fulfillment of the requirements for the degree of

MASTERS OF SCIENCE
in
INDUSTRIAL ENGINEERING

UNIVERSITY OF PUERTO RICO
MAYAGÜEZ CAMPUS
2012

Approved by:

Marcelo Suárez, PhD
Member, Graduate Committee

Date

Viviana Cesaní, PhD
Member, Graduate Committee

Date

José M. Castro, PhD
Co-President, Graduate Committee

Date

Mauricio Cabrera-Ríos, PhD
President, Graduate Committee

Date

Rosario de los A. Ortiz-Rodríguez, PhD
Representative of Graduate Studies

Date

Viviana Cesaní, PhD
Chairperson of the Department

Date

ABSTRACT

In this work, multiple criteria in conflict are considered simultaneously to determine a process window for injection molding (IM). The best compromises between criteria are identified through the direct application of the concept of Pareto-dominance in multiple criteria optimization. With previous information, the translation of the solutions to a graphical representation is carried out for build multiple criteria process window for IM process. This representation will be easier to handle and understand for molders in manufacturing plants. The aim with this work is to provide a formal and realistic strategy to set processing conditions in IM operations. In order to keep the main ideas manageable, the development of the strategy is constrained to two controllable variables in computer simulated parts. As an extension of the method three criteria are incorporated to assess the feasibility. The method proposed here in comparison with other optimization technique such as DEA have a better performance, not required hard programming and computational effort. With the direct application of the dominance and Pareto-optimal concept we have the certain of the correct efficient solutions. Based on the results this strategy is feasible, effective and efficient to find the Pareto-efficient frontier and on prescribing competitive processing conditions in IM operations.

RESUMEN

En este trabajo, múltiples criterios en conflicto son considerados simultáneamente para determinar una ventana de proceso para el moldeo por inyección (MI). Los mejores compromisos entre los criterios se identifican a través de la aplicación directa del concepto de Dominancia y Pareto-optimalidad en la optimización de criterios múltiples. Con la información anterior, se lleva a cabo la traducción de las soluciones a una representación grafica para construir ventanas de procesamiento multicriterio para el proceso de MI. Esta representación será de utilidad y fácil manejar para los moldeadores en plantas de manufactura. El objetivo de este trabajo es proporcionar una estrategia formal y realista para establecer las condiciones de procesamiento en las operaciones de mensajería instantánea. A fin de mantener las ideas principales de su uso, el desarrollo de la estrategia se ve limitada a dos variables controlables de las piezas de ordenador de simulación. Como una extensión del método, tres criterios se incorporan para evaluar su viabilidad. El método aquí propuesto en comparación con otra técnica de optimización tal como DEA muestra un mejor rendimiento, no se requiere gran esfuerzo computacional ni de programación. Debido a la aplicación directa del concepto de Dominancia y Pareto-optimalidad tenemos seguridad de las soluciones

eficientes encontradas. Basándose en los resultados, esta estrategia es factible, eficaz y eficiente para encontrar la frontera Pareto-eficiente así como en la prescripción de las condiciones competitivas de procesamiento en operaciones de MI.

ACKNOWLEDGEMENTS

I would like to express my sincere gratitude to my advisor Dr. Mauricio Cabrera Rios for his support, motivation, knowledge and for trust on me and let me be part of this awesome research group. Thanks for helped me and guidance me during all this process. I could not have a better advisor.

I would like to thank for the rest of my thesis committee: Dra. Viviana Cesani, Dr. Marcelo Suarez and Dr. Jose M Castro for be part of this work and for their feedback and comments. Also I want to thank to Dr. Castro for the research internship opportunities in his research group.

Thanks to the University of Puerto Rico, especially to the Industrial Engineering department for their sponsorship. To CREST (center of research in engineering, science and technology) and thanks to the Applie optimization group and BIO-IE Lab.

I sincerely like to thanks with all my heart and love to the best advisers of my life, my parents: Silvia Yanez Saucedo and Everardo Rodriguez Loc. Thanks for being my

parents, for your love, support and guidance, for trust on me and teach me to make my own decisions in my life. Thanks also, for helped me to be the woman and professional that I am now. I love you both so much.

Thanks to the best friends of my life, my brothers: Silvia Karina Rodríguez Yanez, Marlene Carolina Rodriguez Yanez and Everardo Rodriguez Yanez. Thanks for be there always that I need and give me your advice, for trust on me, for your support and for to be the best brothers ever! I love you so much and I have not words to express how much I love you.

During these years I had the opportunity to met wonderful people, especially my masters partners who which I share study, funny and special memories: Patricia, Karla, Alma Paola, Magaly, Melitza, Cynthia, Marioly, Leemary, Katia, Oscar, Orlando, Irving, Gabriel, Rafael, Andy, Joymariel, Matilde, Esmeralda, The BIO-IE lab girls: Jaileen, Raisa, Jorlys, Marilya, Nicole, Joseira, Paloma, Grace, my smaller friends: Anita and Emilio. Thank you all and the rest of the people that I had the pleasure to meet. Thanks for be part of these great years of my life. Paty thanks for your friendship and share special moments with me. Karla thanks for bring me more than your friendship to be there always and for let me met your wonderful family “my Boricua family”. Alma thanks you so much for be my friend and be there always.

Maga thanks for your friendship and your advice (and don't worry I always take notes and for sure I will be your best student, also, Orlando and Alma made part of this knowledge). Mely thanks also for your friendship and the special memories. Katia thanks for your friendship and your advice always. Cynthia and Marioly thanks for your friendship and for all the special moments. Karen and Luz, thanks to be more than my first housemates, for be my friends and to be there and shared especial and unforgettable moments with me.

Table of Contents

ABSTRACT	II
RESUMEN	III
ACKNOWLEDGEMENTS	V
TABLE OF CONTENTS.....	VIII
TABLE LIST	X
FIGURE LIST	XI
1 CHAPTER.....	14
1.1 INTRODUCTION	14
1.2 MOTIVATION	23
1.3 OBJECTIVE.....	23
2 CHAPTER.....	24
2.1 LITERATURE REVIEW	24
3 CHAPTER.....	30
TECHNICAL BACKGROUND	30
3.1 INTRODUCTION	30
3.2 DESIGN OF EXPERIMENTS (DOE)	30
3.2.1 <i>Central Composite Design (CCD)</i>	31
3.3 RESPONSE SURFACE METHODOLOGY (RSM)	33
3.4 MULTIPLE CRITERIA OPTIMIZATION.....	34
4 CHAPTER.....	37
PROPOSED METHOD	37
4.1 INTRODUCTION	37
4.2 PERFORM AN INITIAL DESIGN OF EXPERIMENTS.....	38
4.3 SCALE THE CONTROLLABLE VARIABLES (CVS) AND PERFORMANCE MEASURES (PMS) TO FALL WITHIN - 1 AND 1.....	38
4.4 FIT A METAMODEL PER PM.....	39

4.5	USE THE METAMODELS TO GENERATE PMS' PREDICTIONS IN THE EXPERIMENTAL REGION OF THE CVS. 39	
4.6	FIND THE EFFICIENT FRONTIER USING THE PMS' PREDICTIONS.....	41
4.7	VALIDATION.....	45
	THE SETTINGS PRESCRIBED IN THE PREVIOUS STEP SHOULD BE VALIDATED EXPERIMENTALLY WHEN POSSIBLE TO ESTABLISH THE PREDICTION QUALITY OF THE METAMODELS. FOR THE PURPOSE OF THIS THESIS, VALIDATION WAS CARRIED OUT THROUGH COMPUTER SIMULATION USING MOLDFLOW INSIGHT 2011. THE EQUIDISTANCE POINTS TO SIMULATION WILL BE SELECTED BASED ON THE NUMBER OF POINTS SUITABLE FOR EACH SIMULATION CASE. FOR A REAL EXPERIMENTAL CASE THE CALCULATION VALIDATION ERROR WILL BE CONSTRAINED IN LESS THAN 10% OF ERROR, USING THE NEXT EQUATION: $ERROR = Y (REAL\ VALUE) - \hat{Y} (PREDICTED\ VALUES)$	
4.8	MULTIPLE CRITERIA PROCESS WINDOW.	46
5	CHAPTER.....	47
	RESULTS.....	47
5.1	ASTM STUDY PART.....	47
5.2	CASE 1: MINIMIZE SHRINKAGE AND MINIMIZE TOTAL WEIGHT	50
5.3	CASE 2: MINIMIZE TOTAL WEIGHT AND MINIMIZE CYCLE TIME	60
5.4	CASE 3: MINIMIZE TOTAL WEIGH, MINIMIZE VOLUMETRIC SHRINKAGE AND MINIMIZE CYCLE TIME ..	69
5.5	COMPARISON OF THE PROPOSED METHOD VERSUS DATA ENVELOPMENT ANALYSIS.....	79
6	CHAPTER.....	82
	CONCLUSION AND FUTURE WORK.....	82
7	REFERENCES.....	85
8	APPENDIX A	89
9	APPENDIX B	97
9.1	CASE A	97
9.2	CASE B	100
10	APPENDIX D.....	103
11	APPENDIX D.....	107
12	APPENDIX D.....	109
13	APPENDIX D.....	111

Table List

Figure 4.3-1. Example of a linear transformation.....	38
Table 5.2-1. Initial experimental design for the case 1.....	51
Table 5.3-1. Experimental design for Case 2.....	61
Table 5.4-1. Experimental design for case 3.....	70
Table 8-1. Predicted efficient solutions and simulated efficient solutions of Case 1.....	89
Table 8-2. Predicted efficient solutions and simulated efficient solutions of Case 2.....	91
Table 8-3. Predicted efficient solutions and simulated efficient solutions of Case 3.....	93

Figure List

Figure 1.1-1. Flow of injection molding process.....	16
Figure 1.1-2. Conflicting between criteria.....	17
Figure 1.1-3. Trade off between criteria.....	19
Figure 1.1-4. Single criteria process window representation.....	20
Figure 1.1-5. Multiple criteria process window representation.....	21
Figure 1.1-6. Graphical representation of efficient frontier through a multiple criteria process window.....	22
Figure 3.2-1. Face-centered central composite design.....	32
Figure 3.4-1. Optimization problem considering only one objective.....	35
Figure 4.1-1. Proposed method.....	37
Figure 4.5-1. Process to find the predicted feasible region.....	40
Figure 4.6-1. Individual pairwise comparison considering the optimization direction in the objective function F1.....	42
Figure 4.6-2. Individual pairwise comparison considering the optimization direction in the objective function F2.....	43
Figure 4.6-3. Dominance cone with the decision direction for Min-Max case.....	43
Figure 4.6-4. Pairwise comparison considering simultaneously both objective function F1 and F2.....	44
Figure 4.6-5. Classification of Dominated Set and Efficient Set of solutions.....	45
Figure 5.1-1. ASTM mold part.....	47
Figure 5.2-1. Graph of principal effect of CVs on Total weight for case 1.....	52
Figure 5.2-2. Graph of principal effect of CVs on Volumetric shrinkage for case 1.....	52
Figure 5.2-3. Experimental region of CV's for case 1.....	54
Figure 5.2-4. Predicted feasible region for case 1.....	55
Figure 5.2-5. Predicted Non-Dominated (squares) and dominated set (empty circles) for case 1.....	56
Figure 5.2-6. Predicted efficient set (full circles) and dominated set (empty circles) for case 1.....	56
Figure 5.2-7. Predicted values (empty circles) vs. simulated values (full circles) for case 1.....	57
Figure 5.2-8. Graph with simulated values classified in efficient (full circles) and dominated values (empty circles).....	58
Figure 5.2-9. Multiple criteria process window classified in three areas for case 1.....	59

Figure 5.3-1. Graph of principal effect of CVs in Cycle Time for case 2.....	62
Figure 5.3-2. Graph of principal effect of CVs in Total Weight for case 2.	62
Figure 5.3-3. Experimental region of CVs for case 2.	64
Figure 5.3-4. Predicted feasible region for case 2.....	65
Figure 5.3-5. Predicted Non-Dominated (squares) and dominated set (empty circles) for case 2.	66
Figure 5.3-6. Predicted efficient set (squares) and dominates set (empty circles) for case 2..	66
Figure 5.3-7. Predicted values (empty circles) vs. Simulation validation values (squares) for case 2.....	67
Figure 5.3-8. Multiple criteria process window classified in three areas for Case 2.....	68
Figure 5.4-1. Graph of principal effect of CVs in Total weight for case 3.	71
Figure 5.4-2. Graph of principal effect of CVs in Volumetric shrinkage for case 3.	71
Figure 5.4-3. Graph of principal effect of CVs in Cycle time for case 3.	72
Figure 5.4-4. Experimental region of CVs for case 3.	74
Figure 5.4-5. Predicted feasible region for case 3.....	75
Figure 5.4-6. Predicted Non-Dominated set (full circles) and dominated set (empty circles) for case 3.	76
Figure 5.4-7. Predicted efficient set (full circles) and dominated set (empty circles) for case 3.	76
Figure 5.4-8. Predicted values (empty circles) vs. simulated values (full circles) for case 3..	77
Figure 5.4-9. Multiple criteria process window classified in three areas for Case 3.....	78
Figure 5.5-1. Efficient frontier using DEA solve.....	80
Figure 5.5-2. Efficient frontier using Proposed method.....	81
Figure 9.1-1. CVs classification by 4 position groups.	98
Figure 9.1-2. Dominate CVs after applied the proposed method.	98
Figure 9.1-3. Efficient frontier after applied the proposed method.	99
Figure 9.1-4. Efficient frontier classified in 4 areas.	100
Figure 9.2-1. . CVs classification by 4 position groups.....	101
Figure 9.2-2. Dominate CVs after applied the proposed method case 2.....	101
Figure 9.2-3. Efficient frontier after applied the proposed method case 2.....	102
Figure 9.2-4. Efficient frontier classified in 4 areas.	102
Figure 53. Residual plots of Total weight for case 1. The normal probability plot in the up left side shows that the points are adjusted at the line. The Residual versus fit plot in the up right side, shows that the points are randomly dispersed around the horizontal axis. In the down right side the residual versus order plot shows an independency between runs.	108
Figure 54. Residual plot of Volumetric shrinkage for case 1. The normal probability plot in the up left side shows that the points are adjusted at the line. The Residual versus fit plot in the up right side, shows that the points are randomly dispersed around the horizontal	

axis. In the down right side the residual versus order plot shows an independency between runs.....	108
Figure 55. Residual plot for Cycle time. The normal probability plot in the up left side shows a good adjusted of the points considering the line. The Residual versus fit plot in the up right side, shows that the points are randomly dispersed around the horizontal axis. In the down right side the residual versus order plot shows an independency between runs around the horizontal axis.	110
Figure 56. Residual plot for Total weight. The normal probability plot in the up left side shows that the points are adjusted at the line. The Residual versus fit plot in the up right side, shows that the points are randomly dispersed around the horizontal axis. In the down right side the residual versus order plot shows an independency between runs..	110
Figure 57. Residual plot for Total weight. The normal probability plot in the up left side shows that the points are adjusted at the line. The Residual versus fit plot in the up right side, shows that the points are randomly dispersed around the horizontal axis. In the down right side the residual versus order plot shows an independency between runs..	112
Figure 58. Residual plot for Volumetric shrinkage. The normal probability plot in the up left side shows that the points are adjusted at the line. The Residual versus fit plot in the up right side, shows that the points are randomly dispersed around the horizontal axis, and a not linear distribution, based on the test this data met the equal variance. In the down right side the residual versus order plot shows an independency between runs.	112

1 CHAPTER

1.1 Introduction

Injection molding (IM) is the most important process for the manufacture of polymer product. A critical challenge in this process is how to set the molding conditions to meet multiple quality criteria such as cycle time, shrinkage, total weight, surface roughness, as many others [1–12] [1], [13], [3–12][1], [13], [3–12][1], [13], [3–12][1], [13], [3–12]. Setting molding conditions is further complicated by the fact that the flow of molten polymers is influenced simultaneously by multiple variables. Setting IM process variables is not trivial, since the physics and chemistry of polymers are tightly coupled and one change in a particular controllable variable geared to improve one quality criterion is often detrimental to another one, i.e. a conflict exists. A process window is a graphical representation that typically involves two processing controllable variables and a response or criterion. The idea is to have a map to determine processing conditions to achieve a desired level of performance by the selected criterion. In this work, two criteria in conflict are considered simultaneously to determine a process window for injection molding. The best

compromises between both criteria are identified through the direct application of the concept of Pareto-dominance. In order to build the proposed strategy, computer simulation of the IM process is used, and real experiments using an IM machine available in The Ohio State University.

The IM process is, indeed, the most important and versatile process for mass-producing thermoplastic products [14], [15]. Injection molded parts can be found everywhere in daily life in automotive parts, packing products, household articles, electronics, and toys-among many others. In general, in IM, plastic pellets are fed into a heated barrel with a reciprocating screw inside that transports the material along the barrel while melting occurs, as shown in Figure 1-1. Under pressure and high temperature, the material is forced into a mold cavity (i). When the plastic parts cools off and solidifies (ii, iii, iv), the mold is open to finally eject the part (v). The five basic stages of the molding cycle are: (i) filling (ii) packing (iii) holding (iv) cooling and (v) ejection as shown in Figure 1-1-1.

INPUT

PROCESS

OUTPUT

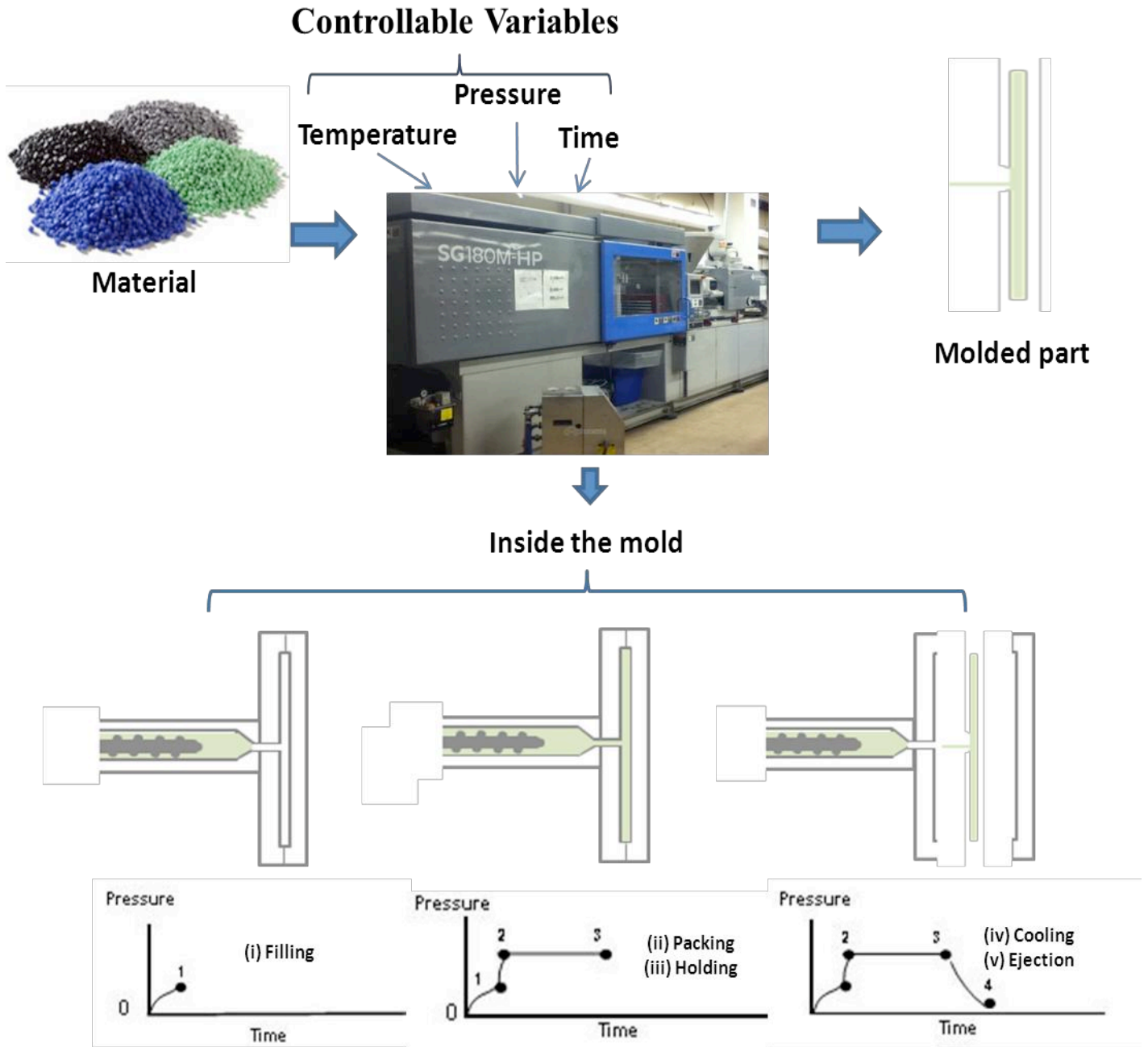


Figure 1.1-1. Flow of injection molding process.

IM parts are typically evaluated considering multiple criteria that are frequently in conflict. This thesis considers two of them simultaneously.

Out of the many possible criteria to consider, cycle time is important in terms of economics, while others like part shrinkage, part thickness and total weight are common proxies for part quality. The effect of different processing conditions on shrinkage, warpage, cycle time and weight of the part have been reviewed in [5], [10], [16–21]. These works mostly consider a single criterion for process improvement. This however, is not realistic in presence of conflict, as it happens in IM and several other manufacturing processes. A conflict between two criteria is illustrated in Figure 1.1-2. Notice that if both criteria are to be minimized, the dark (blue) areas in Figure 1.1-2 must be targeted. This will lead to regions containing combinations of controllable variables that do not overlap, thus evidencing a conflict.

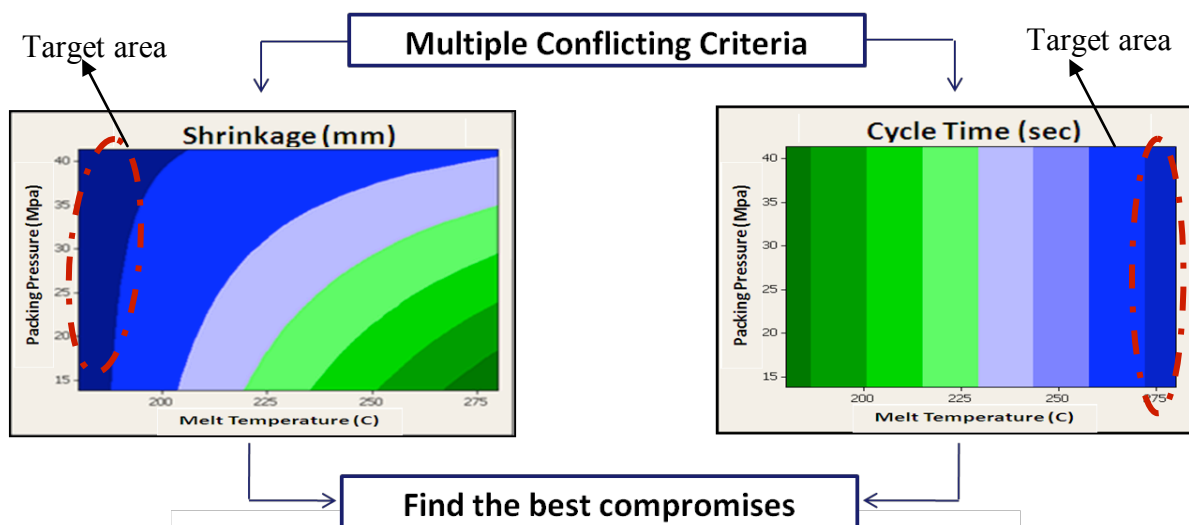


Figure 1.1-2. Conflicting between criteria.

Although it is possible to establish a path from one attractive region to the other, the number of possible combinations is infinite if the controllable variables are continuous or possibly very large if they are discrete.

The information on Figure 1.1-2 can be presented also in the space defined by the criteria under consideration as schematically shown in Figure 1.1-3. In this figure, the desired criterion of both criteria minimization of F1-(cycle time) and F2-(shrinkage), are respectively shown with arrows. The cone formed by the linear convex combinations of the desired directions establishes a region of dominance. Any solution in that region dominates a solution situated in the origin of the cone. A Pareto-efficient (or simply, efficient) solution is found when it originates an empty cone. The set of efficient solutions of the two-criteria optimization problem forms its efficient frontier. Moving from one efficient solution to another implies improving in one criterion but necessarily losing in the other one. In Figure 1.1-3, notice that improving in both criteria is possible only if the cone defining the region of dominance is nonempty.

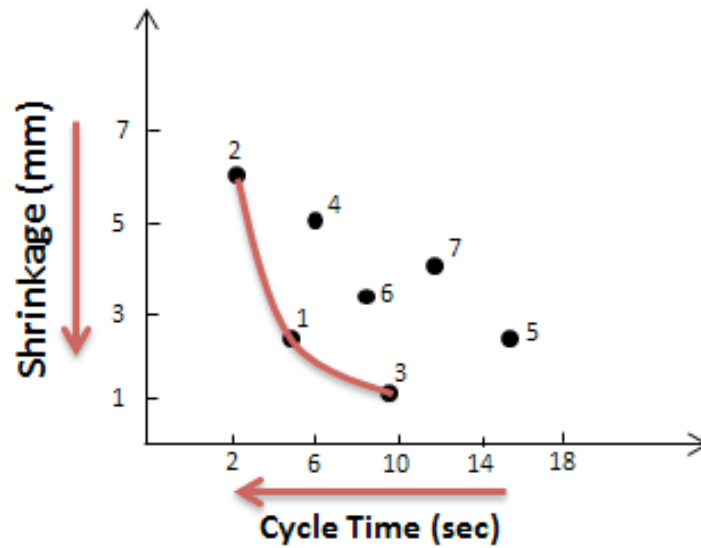


Figure 1.1-3. Trade off between criteria.

In this work, it is proposed to solve bicriteria optimization problems associated to IM to determine their efficient frontier, aiming to make this information available for pertinent decision-making regarding the control of the process.

The results associated with the efficient frontier need to be easily available to the molder for it to be usable. The typical representation of a process window is a graph where one can observe the response surface of a performance measure (PM) of interest and the associated controllable variable values, as shown in Fig. 1.1-4 considering a single criterion and Figure 1.1-5 shown the PW considering multiple criteria. The representation of a multiple criteria process window in IM is not common in the literature review [22], [23]. In this work, the process window is

presented considering two controllable variables and two performance measures as a first approach.

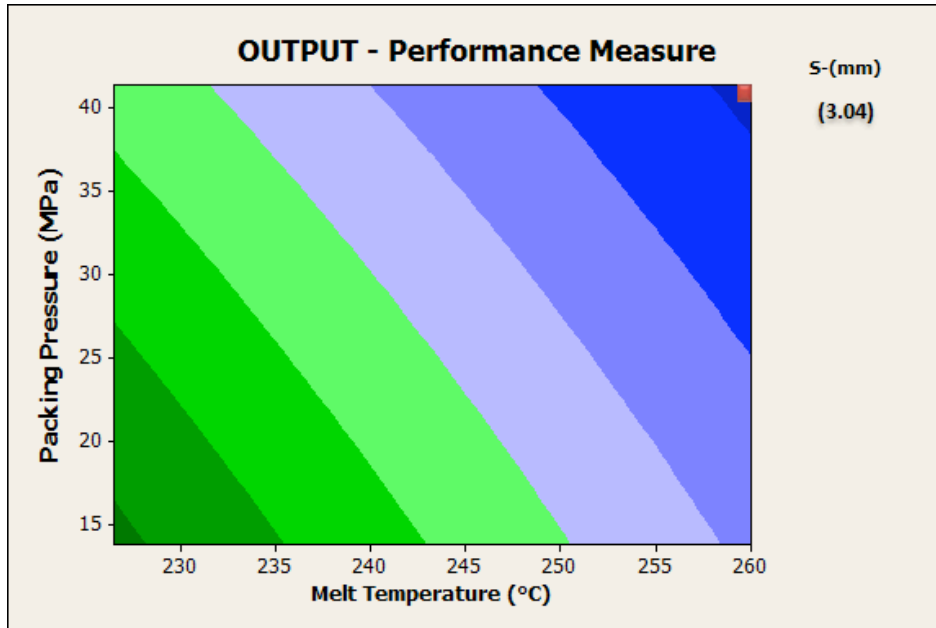


Figure 1.1-4. Single criteria process window representation.

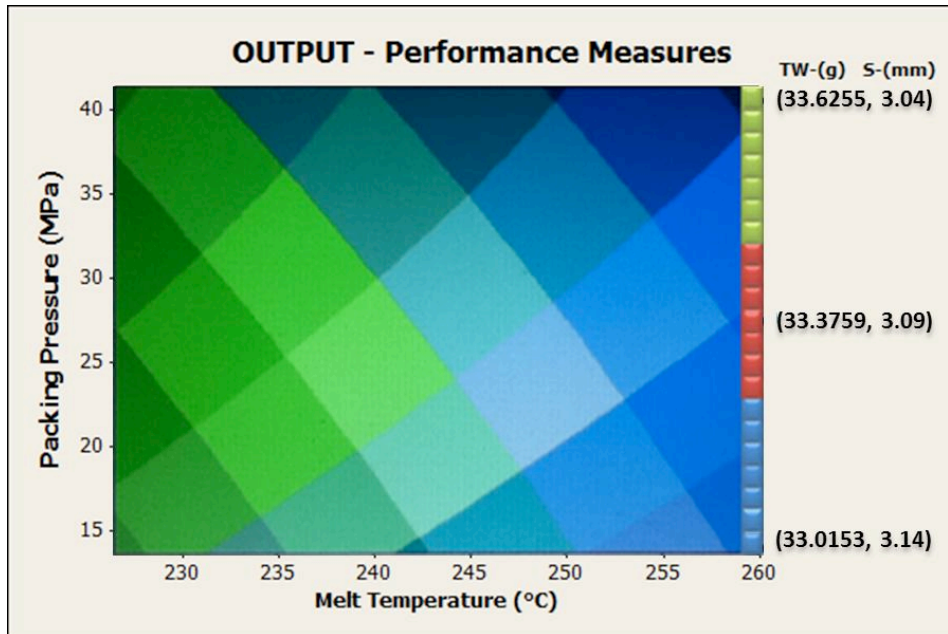


Figure 1.1-5. Multiple criteria process window representation.

Figure 1.1-5 shows two contour plots superimposed one on top of the other. Each contour plot corresponds to a particular PM. Each PM is to be minimized. The axes represent the controllable variables in the IM machine. The efficient frontier, in this particular case, is located in the right hand side of the window, spanning solutions between the attractive areas to each PM.

With the representation shown in Figure 1.1-5, a molder can setup the process knowing the kind of compromise attained in the performance measures involved. An easier-to-read version of the process window is shown in Figure 1.1-6.

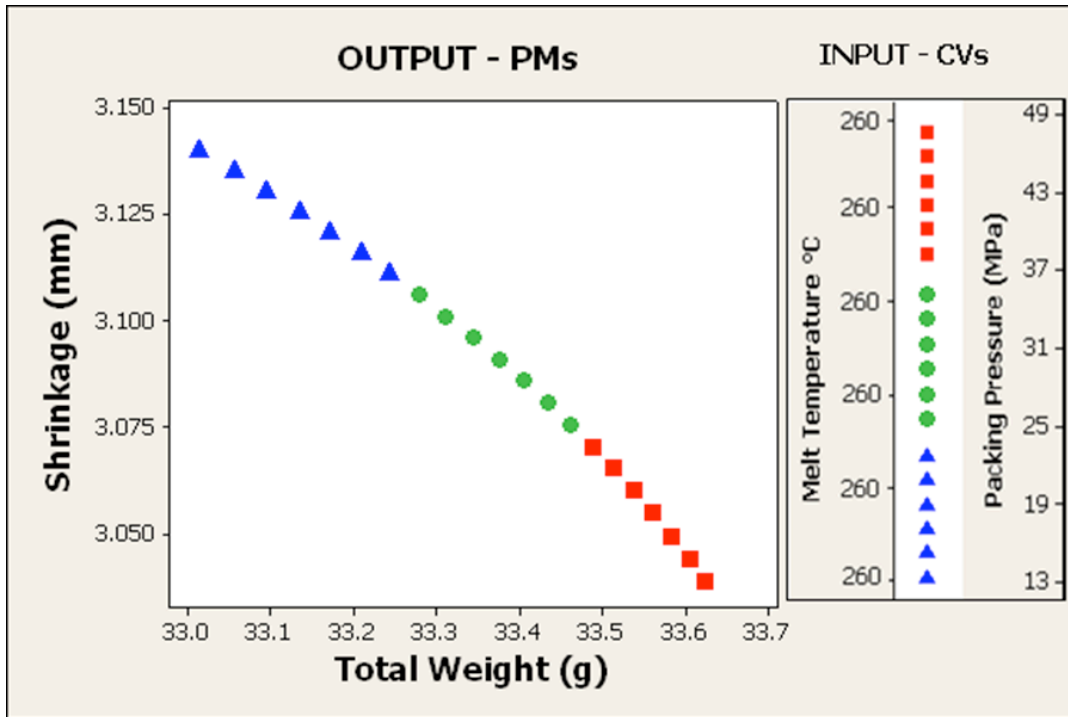


Figure 1.1-6. Graphical representation of efficient frontier through a multiple criteria process window

It is clear that having more than two performance measures would complicate a representation similar to Figure 1.1.5, however, this work presents a first approach to organize multiple criteria information relying in the fact that cases with two performance measures and two controllable variables abound in reality.

1.2 Motivation

Manufacturing plants with IM machines everywhere in the world need to meet all parts' specifications while keeping the operation cost-effective. This challenge is often left to the experience and intuition of process engineers and operators. This process is often cumbersome, lengthy and nonrepeatable, as it heavily relies on trial-and-error. Furthermore, controlling an IM process is complicated by the existence of conflict between multiple performance criteria. This complication makes it unrealistic to consider solely one criterion to set up the IM process. A multiple criteria process window, with clear trade-off information between these criteria, would help circumvent many of the difficulties described here.

1.3 Objective

Develop a method to build process windows under multiple and conflicting criteria to set the processing conditions in IM operations in a consistent and competitive manner. It will also be sought to use a conservative number of runs in the construction of such process window. The aim of this thesis is start such development by considering the two criteria and two controllable variables case in injection molding through the use of simulations.

2 CHAPTER

2.1 Literature review

Many process variables have effects on the quality characteristics of an IM part. When varied simultaneously, not all of these effects are desirable, thereby creating conflicts. The four basic categories in which IM process variables are usually grouped are: temperature-related, pressure-related, time-related and distance-related [15]. IM is used for high production volume of complex parts with potentially tight tolerances. Applications are common in toys, automotive parts, electronic components, and medical and pharmaceutical devices, among others. Several works in the literature present interesting analysis of IM conditions as discussed next.

Design of Experiments (DOE) has become a popular tool to set IM process conditions. DOE is a methodology aimed to carry out an experiment in a way such that appropriate data can be collected to be analyzed through statistical methods, resulting in valid, repeatable and objective conclusions [24]. A DOE can be used to determine the effect of process settings in different IM performance measures (PMs) such as shrinkage, warpage, process cycle time, maximum injection pressure inside the mold, total part weight, among others. The fractional factorial design, for example, has been applied as an initial screening approach to determine which

process variables are important to control relevant PMs in IM [21], [25], [26], as well as in several other manufacturing process [27], [28]. To the same end, the orthogonal array design has been used by the practitioners of Taguchi methods in IM [5], [10], [17], [18], [29]. DOE has also been used to carry out material characterization as in the studies presented in [29], [30]. It is sound to use DOE as a means to detect important process variables. Especial care, however, must be exercised on selecting an adequate design to a particular objective because it plays an important role on the capabilities of any DOE study.

Optimization is another concern associated with IM process. Optimization in the related literature is widely understood as the manipulation of controllable variables to improve the performance of a system. In its most complete sense, optimization entails providing evidence of the dominance of a particular configuration of the system over all possible configurations. Several IM optimization endeavors can be found in the literature approached with several kinds of techniques [3], [5], [6], [9], [11], [13], [23]. These works are further categorized below.

IM optimization is often times approached focusing on a single criterion or PM. Using a sequence of an initial experimental design and an empirical model such as a regression equation, an artificial neural network or a kriging model are also frequently used strategies. In [5], an optimization methodology based on Artificial Neural Networks (ANNs) and genetic algorithms (GA) aims to minimize the warpage

of an injection molding part using Moldflow simulations. The ANN is used to model part warpage as a function of mold and melt temperature, packing pressure, packing time, cooling time as well as gate location and runner type. A GA is then used to find the minimum warpage based on the ANN approximation. A somewhat similar approach using ANNs and GAs was presented in [16] focusing on the optimization of part weight. Minimizing a part's volumetric shrinkage through the use of regression and steepest descent was the subject of a study presented in [3] based on simulations and experimental validation runs. A strategy with a kriging model and global optimization techniques is presented in [31] to reduce part warpage. From these works, it is notorious how the use of empirical models –fit through a well-crafted DOE-can be advantageous to expedite an optimization procedure. The fact that IM involves many PMs that show conflict, however, renders the use of a single criterion insufficient to realistically represent the decision making involved on setting process conditions.

When considering multiple conflicting criteria in simultaneous optimization, there is not a single optimum solution, but rather, a series of best compromises or trade-off solutions [32]. These solutions are called Efficient solutions (Pareto-efficient, formally), and form the efficient frontier of a multiple criteria optimization problem. Multiple criteria optimization has actually been considered in various works, including [6], [9], [11], [23], [33–38]. One particularly interesting coincidence in these works is the use of artificial intelligence methods to approach the optimization task.

Several variations of multiple-objective GAs and Evolutionary Algorithms (EAs) are used across these works to determine the best compromises on a number of criteria. GAs and EAs fall into the category of metaheuristics and have, indeed, showed to be very competitive in finding efficient solutions. Their effective use, however, does imply setting a series of parameters by the user that affect the final solution. The challenge of choosing a particular efficient solution over another is not approached in many of these works, irrespectively of the technique used. A process window that captures at least two PMs and helps to choose a particular set of conditions would be an initial way to cover this area.

In recognition of the limitations of several multiple criteria optimization representations [39] and the not-completely solved task of selecting among several efficient solutions, in [40] an approach to involve the preferences in an evolutionary algorithm is presented to then make use of Pareto-optimality conditions to arrive to a final decision. Because the output of a multiple criteria optimization problem is multidimensional, its representation is difficult and thus, its use might not be straightforward. For this reason, a multiple criteria process window could prove useful too.

Our research group has advocated the use of Data Envelopment Analysis (DEA) for multiple criteria optimization in polymer processes [9], [22], [33], [36], [41]. The analyses strategies capitalize on DOE, empirical modeling and DEA. DEA has the

advantage of finding efficient solutions through the use of a series of linear optimization problems, which is very computationally convenient. Furthermore, the solutions found through DEA are undoubtedly Pareto-efficient, which makes it an exact method (non-heuristic). The efficient frontier identified through DEA, however, is often times constrained to convexity. If the true efficient frontier of a multiple criteria optimization problem is not convex, then several efficient solutions might escape detection through DEA. An idea proposed previously in our group entailed using additional optimization problems to detect the efficient solutions lying in nonconvex regions with success, however, it is still a somewhat elaborated process [22]. The work in [22], along with its graphical representation of multiple criteria process window in IM process set the basis for the method proposed in this thesis. For completeness, a review of single-criterion process window works can be found in [42].

In summary, from the literature review it is clear that setting the process conditions in IM is truly a multiple criteria optimization problem that requires, however, a representation that allows translating its solution to information that is easy to handle for molders in manufacturing plants. This challenge motivates the work in this thesis, where the proposed method to build process windows under multiple and conflicting criteria to set the processing conditions in IM operations in a consistent and competitive manner is presented. Previous works in literature review used different optimization techniques that required hard computational and programming work and

due the heuristic predictions the certain of the optimal solution is not 100%. The method proposed here in comparison with other optimization technique such a DEA have a better performance, not required hard programing and computational effort and also, due the direct application of the dominance and Pareto-optimal concept we have the certain of the correct efficient solutions.

3 CHAPTER

TECHNICAL BACKGROUND

3.1 Introduction

In this chapter, a brief explanation of the different techniques that integrate the proposed method is presented. First, the focus is on design of experiments as a central technique to obtain data that is statistically valid. Then, regression metamodeling is described to finally introduce the concept of Pareto-efficiency.

3.2 Design of experiments (DOE)

DOE has become a popular tool to set IM process conditions. Researches perform experiments usually to study the performance of a particular process or system under controlled conditions. DOE is defined as series of tests in which purposeful changes are made to the controllable variables of a process or system so that we may observe and identify the reasons for changes that may characterize and model their effect on response variables of interest [24].

DOE involves all phases of experimentation: planning, execution, analysis and conclusion. Planning and experiment includes defining the objective of the study as

well as establishing all parts of the system under consideration. With knowledge about the system and objective, then it is possible to choose a statistical design with an adequate number of runs, replicates, and combination on the levels of the factors to be controlled and measured in the experiment.

The execution of the experiment is supposed to follow the plan as close as possible, or else to make any deviation explicit for accounting purposes. Once with the experiment, the plan also dictates the statistical analysis associated to the objective. The results are finally translated into conclusions. This is usually followed by a new experiment round with a new objective. In this work, a DOE is used to build regression models (metamodels). To this end, the central composite design (CCD) is introduced next as a preferable design of choice.

3.2.1 Central Composite Design (CCD)

For the purposes of the proposed method, a **central composite design** or **CCD** is recommended. CCD is the most popular design used to fit a second-order regression model. The **CCD** for k factors consists of a 2^k factorial design with 2^k runs, $2k$ axial or star runs, and n_c center runs (n_c is usually between 3 and 6). An example of face-centered central composite design is shown in Figure 3.2-1.

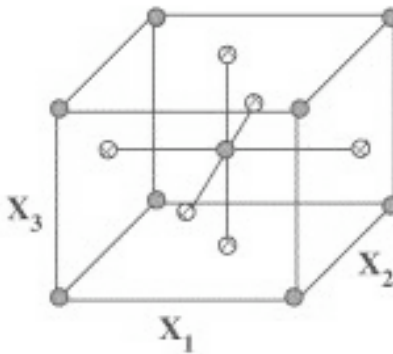


Figure 3.2-1. Face-centered central composite design.

The CCD needs can be carried out sequentially or in “one shot”. The CCD is an economic design with proven qualities for metamodeling including balance, keeping similar variance in regression coefficients, and capability to estimate curvature. When a CCD cannot be used, Z-level or 3-level factorials are alternatives, although these should not be the first choices.

In general, if a single dependent or response variable y that depends on k independent or controllable variables, x_1, x_2, \dots, x_k , the relationship between these variables can be characterized by a mathematical model called **regression model**. This model expresses the results of an experiment quantitatively in terms of **statistical model** that facilitates understanding, interpretation, and implementation of particular solutions. To this end, it is important to know some basics on response surface methodology.

3.3 Response surface methodology (RSM)

Response surface methodology or **RSM** is a collection of mathematical and statistical techniques useful for the modeling and analysis of problems in which a response of interest is influenced by several variables and the objective is to optimize this response [24]. In most RSM problems, the form of the relationship between the response and the independent variables are unknown. RSM is used first to find the suitable approximation for the true functional relationship between y and the set of independent variables.

For the purposes of this thesis, a polynomial of second degree must be used, such as the **second-order regression model**. Let us consider the model represented by:

$$(2-1)$$

The parameters β_j 's represent the regression coefficients. y_{ij} represent the values of the variable y (at the eth experimental point. And the ϵ_{ij} represent the uncorrelated random error with mean zero and variance σ^2 .

The second order regression metamodels are used to approximate performance measures. The quality of these metamodels is very important. In the proposed

method, having an R^2 value of at least 90% is a good rule of thumb for each metamodel.

3.4 Multiple criteria optimization

Optimization is an important technique to make any process more effective and efficient. An optimization problem refers to finding one or more feasible solutions that correspond to the best possible values for one or more criteria. In the real world is common to find optimization problems with more than one criterion that must be satisfied simultaneously. Thus, considering only one criterion when multiple criteria exist as in Figure 3.4-1, is not realistic.

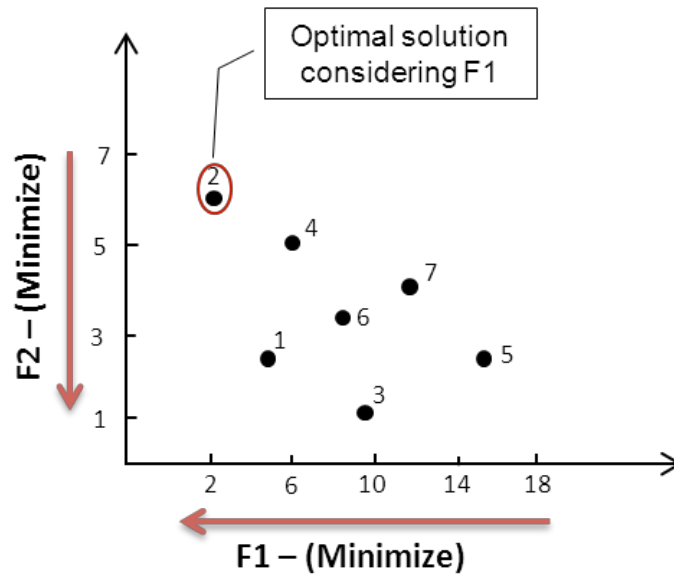


Figure 3.4-1. Optimization problem considering only one objective.

Considering more than one objective function to find optimal solutions is known as *multi-objective optimization*. This kind of problems is considered part of multicriteria optimization and then of multicriteria decision-making (MCDM).

In this kind of problems, the goal is to find the set of best compromises or “trade-offs” between the different criteria as shown in Figure 3.4-2.

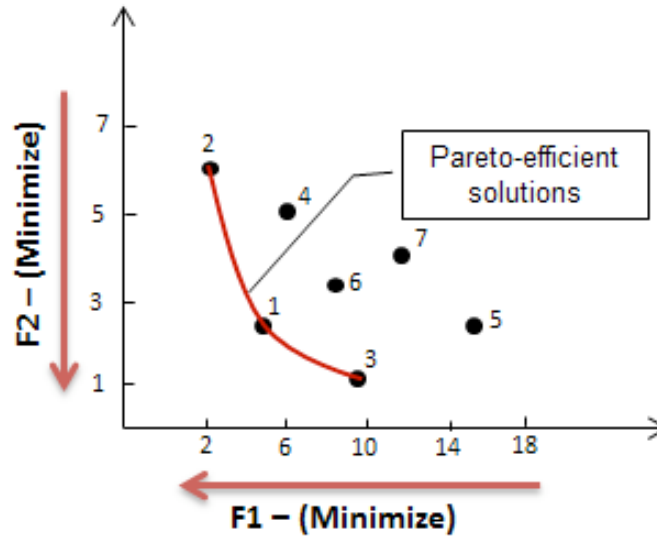


Figure 3.4-2. Optimization problem considering simultaneously two objectives.

The best compromises, as it was said previously, are called Efficient solutions (Pareto-efficient, formally) and form the efficient frontier of multiple criteria optimization problem.

4 CHAPTER

PROPOSED METHOD

4.1 Introduction

The method proposed to build a multiple criteria process window for IM is shown in Figure 4.1-1.

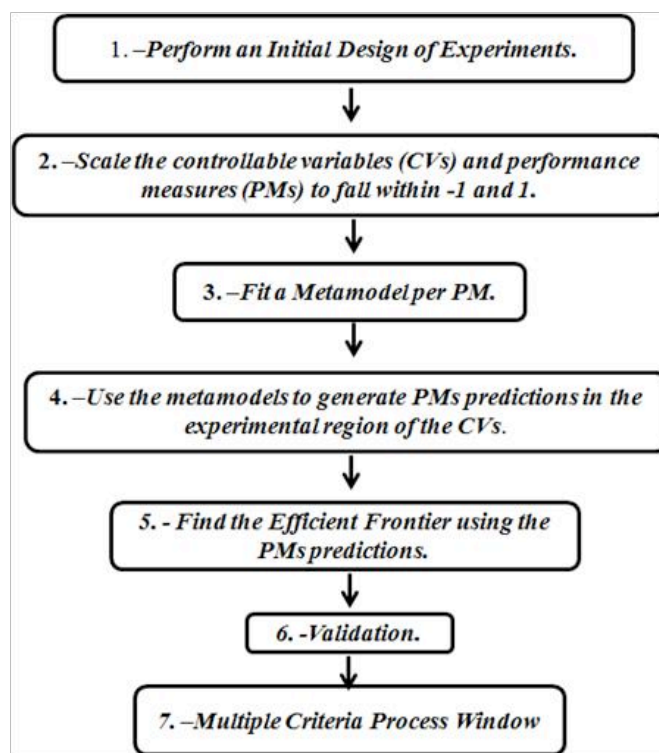


Figure 4.1-1. Proposed method.

This method integrates different techniques such as Design of Experiments and Multiple Criteria Optimization. The organization is described in the following steps:

4.2 Perform an initial design of experiments.

The initial design of experiments must be able to provide data to correctly build a second order regression model. For the purpose of this method, the use of a central composite design is highly advised. In the case presented here the responses will be obtained through computer simulations, however, it is envisioned that experimental runs be used in the near future.

4.3 Scale the controllable variables (CVs) and performance measures (PMs) to fall within -1 and 1.

Each CV and PM must be in the same scale. This is accomplished through suitable linear transformations, as shown in Figure 4.3-1.

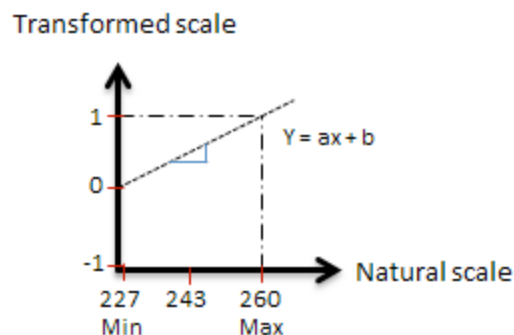


Figure 4.3-1. Example of a linear transformation.

4.4 Fit a Metamodel per PM.

The scaled data are used to generate second order regression metamodels. It is important that the fit corresponds to an R-Sq \geq 90% on each metamodel.

4.5 Use the metamodels to generate PMs' predictions in the experimental region of the CVs.

PMs' predictions are obtained following a factorial grid on the experimental region of the CVs. Each point in the grid corresponds to a particular combination of CVs' values. Figure 4.5-1 shows the process used in this thesis to map-out the feasible region as explained below:

(1) Varying from -1 to 1 in increments of 0.01 on each CVs, the total number of combinations are $(21 \text{ values per CV} = 21^2) = 441$ combinations. (2) The values of each combination are used to generate PM predictions. (3) The predictions, which are also pairs of values, are plotted. Finally the feasible region between two conflicting criteria is apparent.

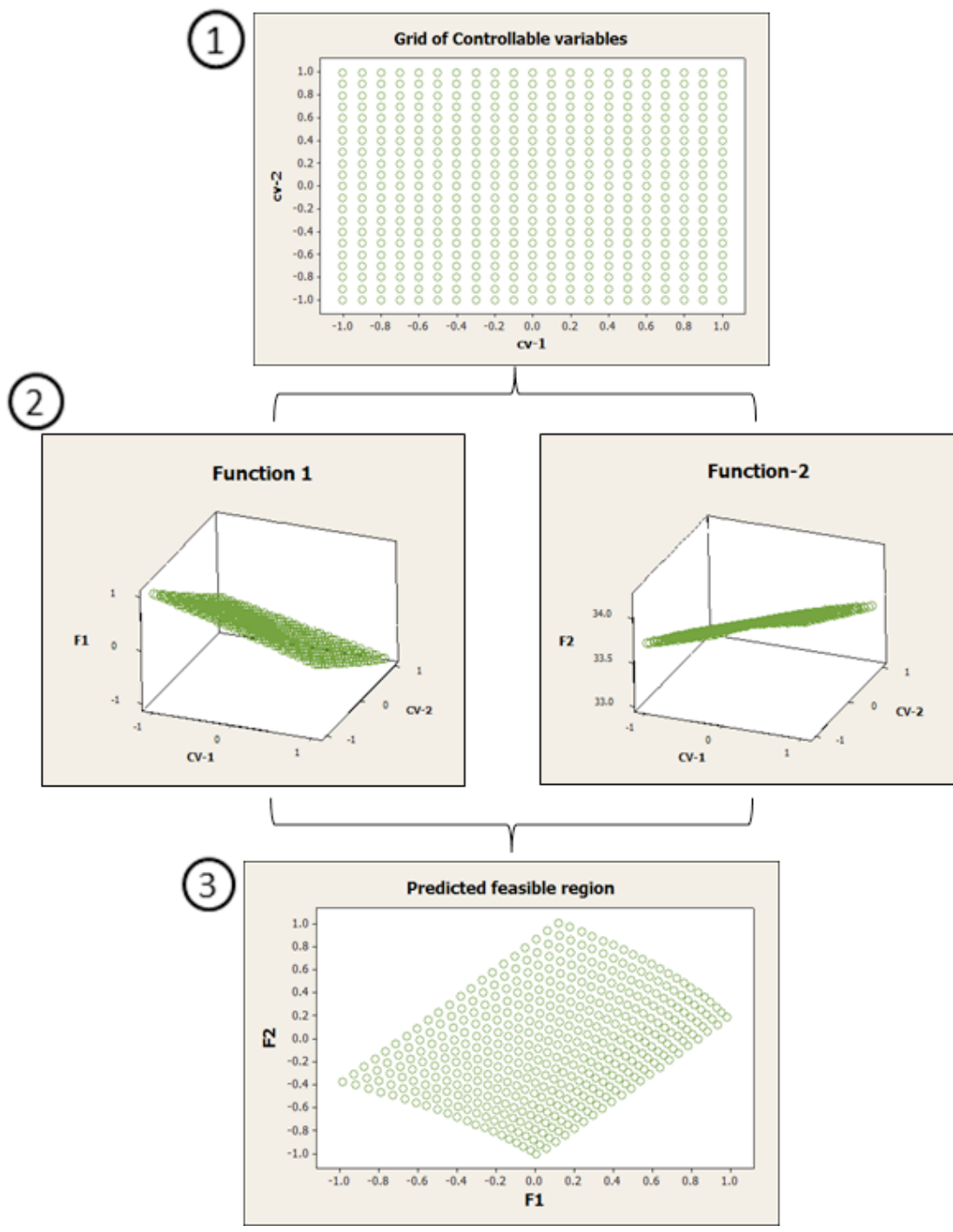


Figure 4.5-1. Process to find the predicted feasible region.

4.6 Find the Efficient Frontier using the PMs' predictions.

The PMs' predictions are used to make pairwise comparisons among all grid points. The best compromises between the two criteria are identified through the application of two conditions as described next.

The operator \succcurlyeq is used to denote (no worse than), and the operator \prec to denote (better than).

Definition 1) The solution $X(1)$ is no worse than $X(2)$ in all objectives, or $f_j(X(1)) \succcurlyeq f_j(X(2))$ for all $j=1, 2, \dots, M$.

Definition 2) The solution $X(1)$ is strictly better than $X(2)$ in at least one objective, or $f_j(X(1)) \prec f_j(X(2))$ for at least one $j \in \{1, 2, \dots, M\}$.

The points that meet conditions 1 and 2 are considered Pareto efficient and are thus the best compromises between the PMs. The combinations of values of the CVs associated to the efficient solutions are said to dominate the rest of the set. After this step, the Efficient Frontier and their associated processing conditions are identified.

To illustrate the application of the concept represented by definitions (1) and (2), Figures 4.6-1 and 4.6-2 are considered. Seven solutions are presented in the space defined by two criteria, F1 and F2, the first which is to be maximized while the second one must be minimized. In Figure 4.6-1, the solution with maximum value in F1 is found, and in Figure 4.6-2 the solution with the minimum value in F2 is found. The process to find these solutions is to perform an exhaustive pairwise comparison among all solutions.

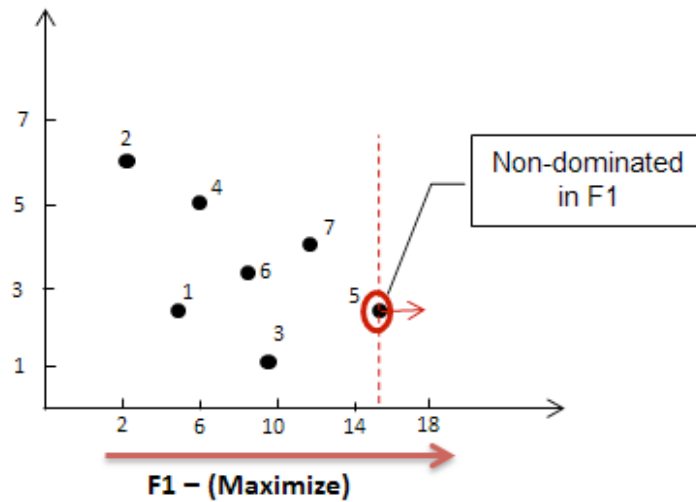


Figure 4.6-1. Individual pairwise comparison considering the optimization direction in the objective function F1.

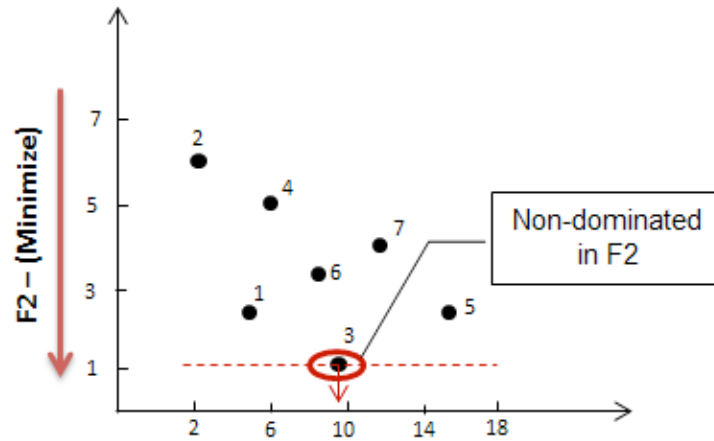


Figure 4.6-2. Individual pairwise comparison considering the optimization direction in the objective function F2.

In order to find the best compromises between F1 and F2, the cone defined by the optimization direction of these criteria is considered. This cone is illustrated in Figure 4.6-3. A solution resting at the origin of this cone is dominated by any solution within the cone. A solution resting at the origin of this cone is efficient if and only if this cone is empty. Thus, this cone is, conceptually, a dominance cone.

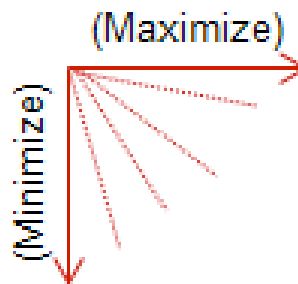


Figure 4.6-3. Dominance cone with the decision direction for Min-Max case.

Figure 4.6-4 shows the application of definitions (1) and (2). If solution 2 is placed at the origin of a dominance cone, many solutions are found within it and, therefore solution 2 is a dominated solution. In the other hand, when solution 5 is analyzed, an empty dominance cone is found. Solution 5 is, then an efficient solution. Figure 4.6-5 shows the sets of dominated and efficient solutions in this example.

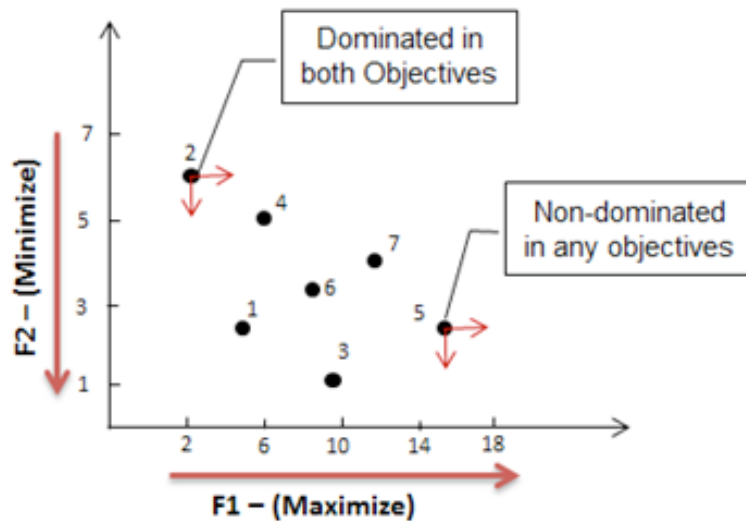


Figure 4.6-4. Pairwise comparison considering simultaneously both objective function F1 and F2.

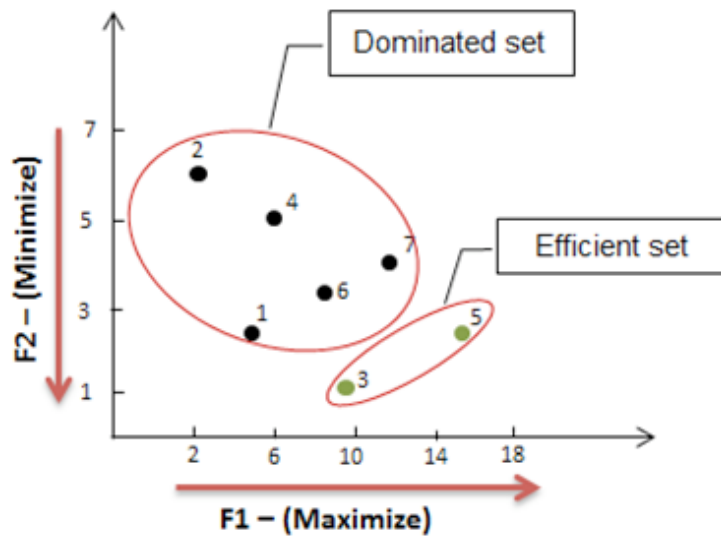


Figure 4.6-5. Classification of Dominated Set and Efficient Set of solutions.

Once the efficient set has been identified, these solutions can be traced back to their corresponding processing conditions. This process effectively ties IM performance to the controllable variables.

4.7 Validation.

The settings prescribed in the previous step should be validated experimentally when possible to establish the prediction quality of the metamodels. For the purpose of this thesis, validation was carried out through computer simulation using Moldflow Insight 2011. The equidistance points to simulation will be selected based on the number of points suitable for each simulation case. For a real experimental case the calculation validation error will be constrained in less than 10% of error, using the next equation: $error = y (real\ value) - \hat{y} (predicted\ values)$

4.8 Multiple criteria process window.

The final step shows the results through a graphic tool. The typical representation of a process window is a graph where one can observe the response surface of a performance measure (PM) of interest and the associated controllable variable values as illustrated in Chapter 1. The corresponding figure is reproduced here for convenience Figure 1.1-6.

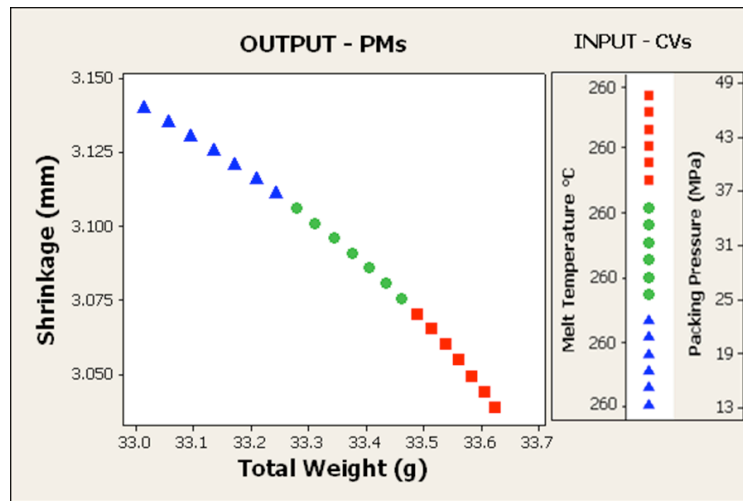


Figure 1.1-6. Graphical representation of efficient frontier through a multiple criteria process window

The application of the proposed method is illustrated through three case studies in the following chapters. The third case evidences the capability of the method to include more than two performance measures. Additionally, a comparison to a well-known multicriteria optimization technique, Data Envelopment Analysis, is presented towards the end of this thesis.

5 CHAPTER

RESULTS

5.1 ASTM study part.

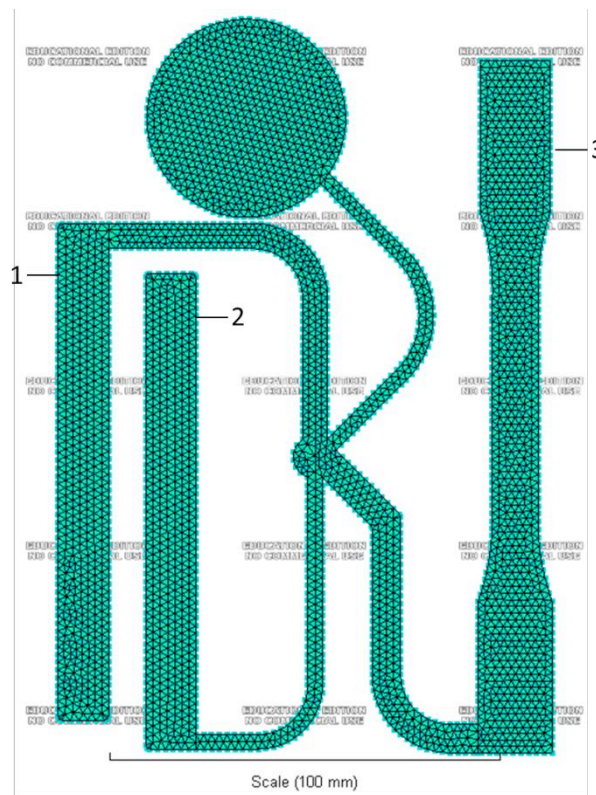


Figure 5.1-1. ASTM mold part.

A mold to produce a part for ASTM (American Society for Testing and Materials) destructive tests, Figure 5.1-1, as an extension, real experiments were carried out at The Ohio State University. The real experiments results are not included in this

thesis. In the meantime, at UPRM the strategy is under development using the finite element mesh of this part and polymer flow simulation software (Moldflow). This part is selected for the simulation and real experiments due the geometric complexity that make more interesting the analysis. The components of ASTM mold part are identified with numbers 1-3: Tensile bar, Thin flex and Thick flex, respectively. To evaluate volumetric shrinkage we consider the percent of the hold mold part. In order to estimate Total Weight³, we considered the entire mold part excluding the sprue, which is the main channel for feeding material into the mold. The Cycle Time was estimated as through the time at which the part was finally demolded. The PMs evaluated in the case studies are explained as follows:

Shrinkage: defined as the difference between the dimension of a molded part and its associated mold dimension. It occurs when polymers cool off.

Volumetric Shrinkage is a fundamental part of the shrinkage calculations. The main factors affecting volumetric shrinkage are pressure and the melt temperature.

Based on the Moldflow software the volumetric shrinkage is calculated as follows:

$$\text{---} \tag{5.1}$$

where v_1 is specific volume of polymer at the time when either the polymer in element becomes completely frozen or melt pressure in the element becomes atmospheric; v_2 is the specific volume of polymer at atmospheric pressure and room temperature. Specific volume at a particular pressure and temperature is calculated using the PVT relationship.

Cycle Time: as it is known high cycle times reduce the productivity and increase the manufacturing costs. Is calculated as follows:

$$T_c = t_{open/close} + t_f + t_c + t_e \quad (5.2)$$

where: $t_{open/close}$ is the time required to open or close the mold before and after part ejection, respectively; t_f is the mold fill time including the packing and holding stages; t_c is the part cooling time after the mold has been filled; and t_e is the part ejection time, [44].

Total Weight: it is known to be a good estimator of part quality but also a cost driver, thus it is considered in the analyses presented here.

5.2 Case 1: Minimize Shrinkage and Minimize Total Weight

The PMs considered in this first case are Total Weight (g) and Volumetric shrinkage (%). Both impact dimensional stability and the quality of molded parts and both must be minimized. The CVs are Packing Pressure and Melt Temperature. These are varied in the ranges [227,260] °C and [13.79, 41.36] MPa respectively. Experimental ranges for the CVs were determined using the recommended values from the material database in Moldflow Insight 2011.

The material chosen was D21148 LyondelBassel Advanced Polyolefin USA Inc. For the case 1 Mold temperature is let constant at 32°C, injection time at 1 sec, V/P Switch at 80%, packing time at 10 sec, and cooling time at 20 sec. In order to obtain a multiple criteria process window the proposed method is followed.

Step 1: Perform an initial design of experiments.

A central composite design involving both variables and both PMs was carried out.

The initial experimental design is shown in Table 5.2-1.

Table 5.2-1. Initial experimental design for the case 1.

Run	Melt Temperature (°C)	Packing Pressure (MPa)	Total Weight (g)	Volumetric Shrinkage (%)
1	227	13.79	33.6981	15.57
2	227	27.58	33.9983	15.24
3	227	41.36	34.2365	15.10
4	243	13.79	33.3561	16.40
5	243	27.58	33.6962	16.13
6	243	41.36	33.9141	16.01
7	260	13.79	33.0058	17.33
8	260	27.58	33.3884	17.17
9	260	41.36	33.6225	17.05

The Figures 5.2-1 and 5.2-2 shows the simulation experimental results graphically.

The following can be observed: an increase in Pp results in an increase in total weight while in volumetric shrinkage, and an increase in melt temperature results in a decrease total weight and an increase in Volumetric shrinkage. Indeed, an increase of Pp seems to benefit Shrinkage while moving Total weight in an undesired direction. An increase of Tm seems benefit total weight but not for volumetric shrinkage because of less material inside the mold, thereby evidencing a conflict.

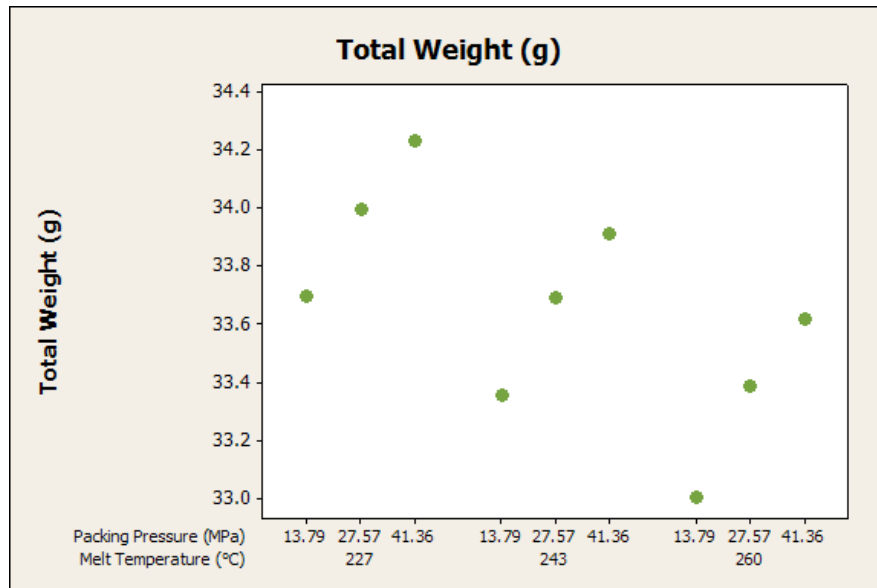


Figure 5.2-1. Graph of principal effect of CVs on Total weight for case 1.

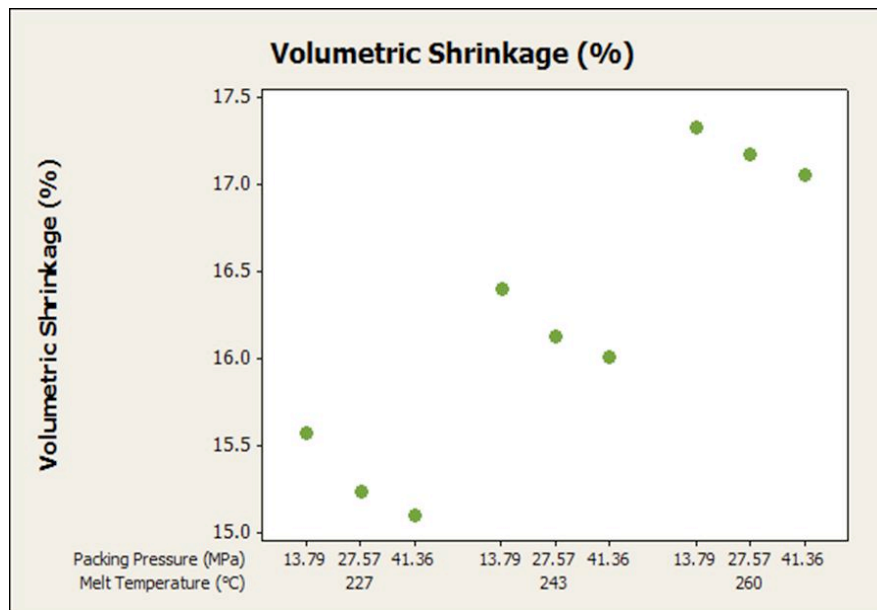


Figure 5.2-2. Graph of principal effect of CVs on Volumetric shrinkage for case 1.

Step 2: Scale the controllable variables (CVs) and performance measures (PMs) to fall within -1 and 1.

Each CV and PM must be between -1 and 1 to avoid dimensionality problem. This is accomplished through a linear transformations.

Step 3: Fit a Metamodel per PM.

The scaled data are used to generate second order regression metamodells. The metamodells were obtained through a response surface regression using Minitab 16. It is important that the fit corresponds to R-Sq \geq 90% on each metamodel. In this case both metamodells met this condition and are presented next:

$$\text{Total Weight} = 0.1158 - 0.5190T_m + 0.4640P_p + 0.0046T_m^2 - 0.0901P_p^2 + 0.0318T_mP_p \quad (5.1-1)$$

$$\text{R-Sq} = 99.93\%$$

$$\text{R-Sq (adj)} = 99.81\%$$

$$\text{Volumetric shrinkage} = -0.0693 + 0.8430T_m - 0.1704P_p + 0.0568T_m^2 + 0.0568P_p^2 + 0.0426T_mP_p \quad (5.1-2)$$

$$\text{R-Sq} = 99.96\%$$

$$\text{R-Sq (adj)} = 99.90\%$$

Where T_m is Melt Temperature and P_p is Packing Pressure. The analysis of variance (ANOVA) of this case study is presented in Appendix 10.

Step 4: Use the metamodels to generate PMs Predictions in the experimental region of the CVs.

The previous second order regression metamodels and 441 combinations of CVs shown in Figure 5.2-3 as a grid were used to predict the values of the PMs and this to find Predicted Feasible Region (PFR) in the space of the criteria.

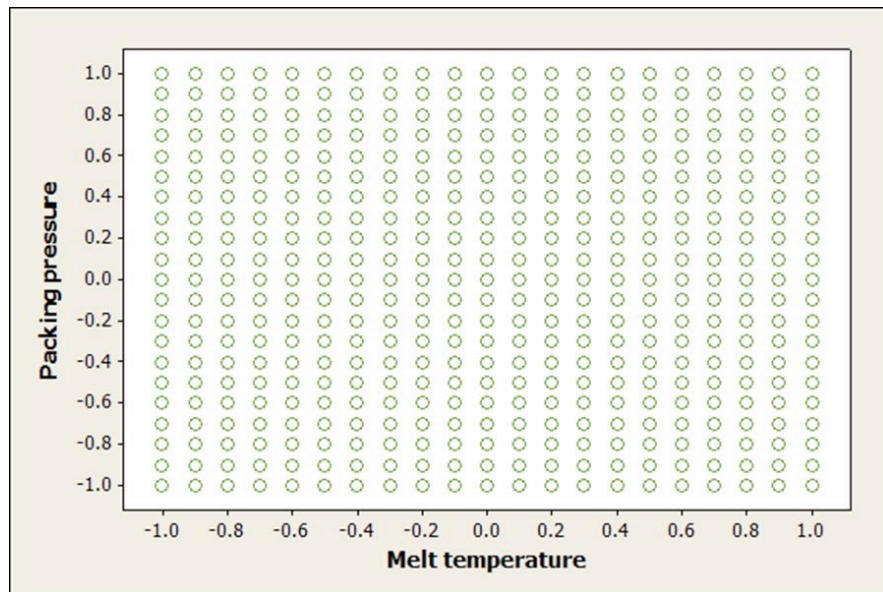


Figure 5.2-3. Experimental region of CV's for case 1.

The 441 combinations correspond to a sampling of 21 levels per CV, which is an arbitrary number at this point. The previous second order regression metamodels and the 441 combinations of CVs were used to predict the values per PMs and find Predicted Feasible Region. The PFR is show in Figure 5.2-4.

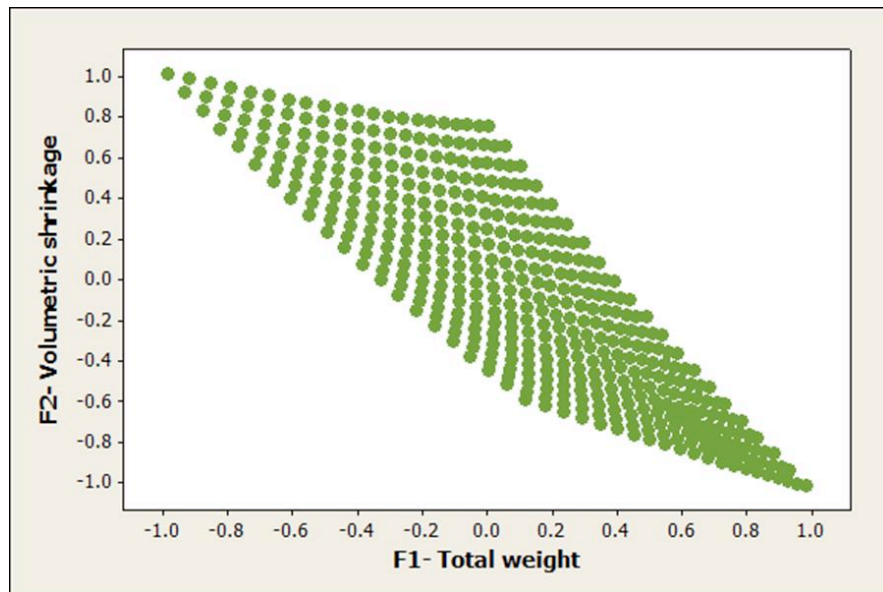


Figure 5.2-4. Predicted feasible region for case 1.

Step 5: Find the Efficient Frontier using the PMs' predictions.

In order to find the Predicted Efficient Solutions (PES) and their associated values of CVs definitions (1) and (2) are applied. The pairwise comparisons were carried out using an Excel spreadsheet. Figure 5.2-5 shows the predicted Non-Dominated set of solutions while Figure 5.2-6 shows the shape of the PFR and the location of PES.

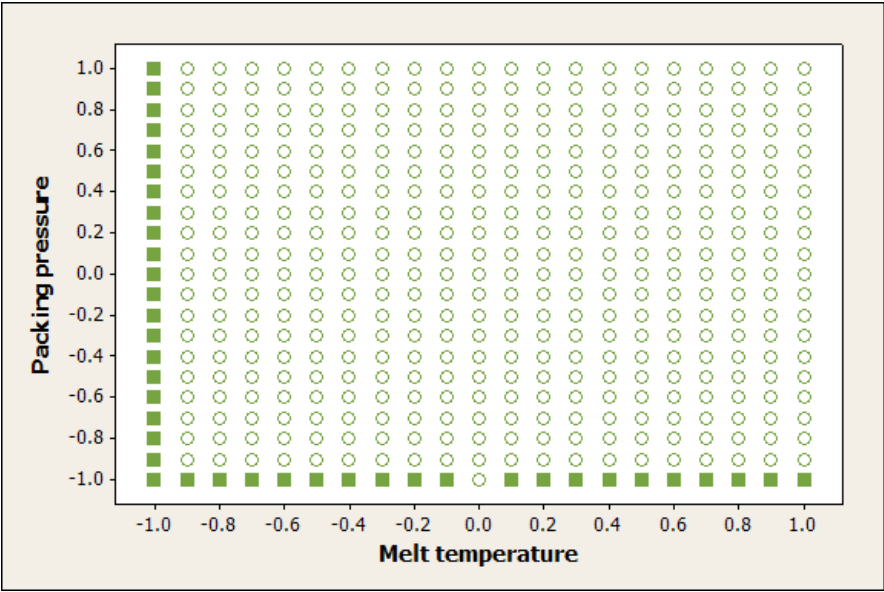


Figure 5.2-5. Predicted Non-Dominated (squares) and dominated set (empty circles) for case 1.

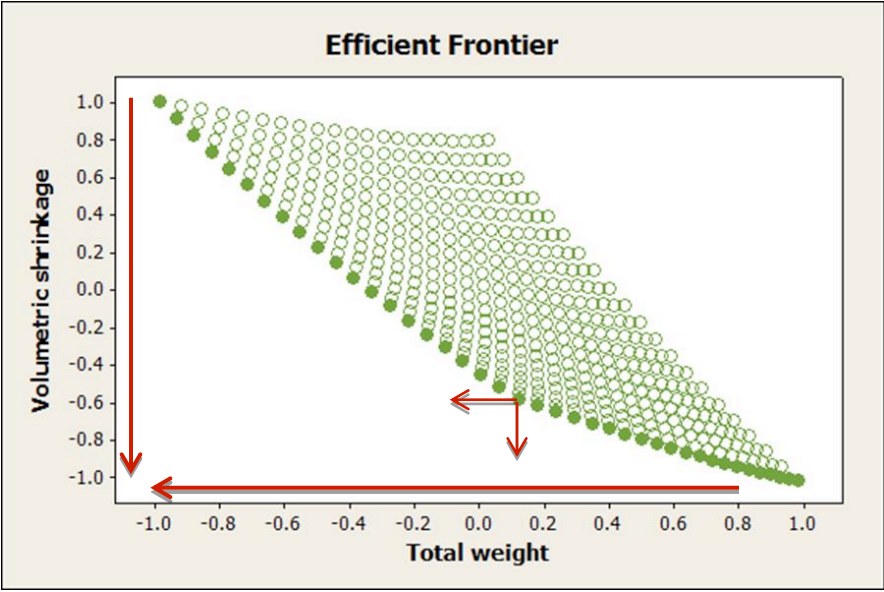


Figure 5.2-6. Predicted efficient set (full circles) and dominated set (empty circles) for case 1.

Step 6: Validation.

All PES were used to perform validation runs. These results are shown in Figure 5.2-7. The associated values of CVs, Predicted Solutions and the results of simulations validations are shown in Table 8.1 in Appendix A.

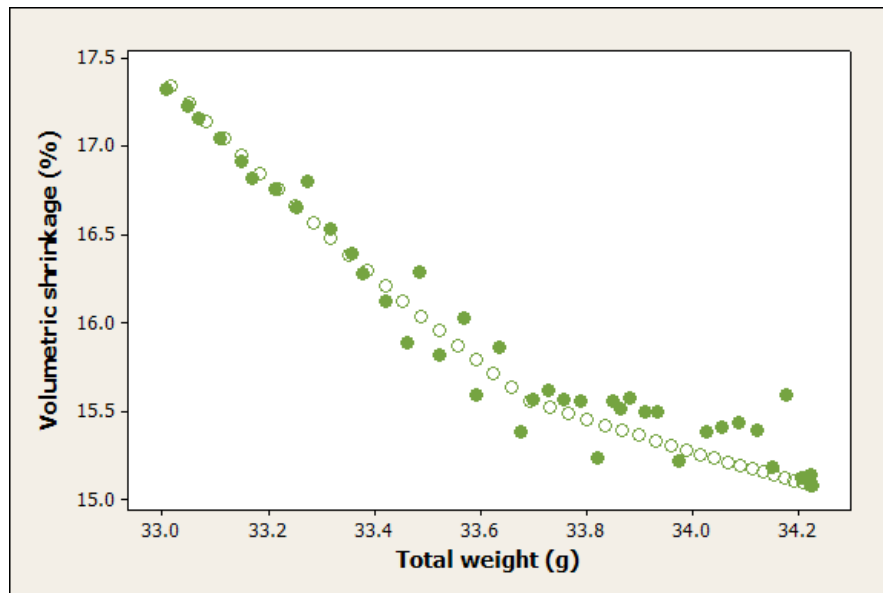


Figure 5.2-7. Predicted values (empty circles) vs. simulated values (full circles) for case 1.

In Figure 5.2-7 shows that there are values within less than 1% of error and there are many others within less than 10% of error. As can observe in figure above the simulated volumetric shrinkage values are higher than the predicted, this performance because of the variable cooling time set at 20 sec.

For other side, if we compared the simulated values, a new real efficient frontier is found. For this particular case, the simulated values were classified in efficient and dominated values as can observe in Figure 5.2-8.

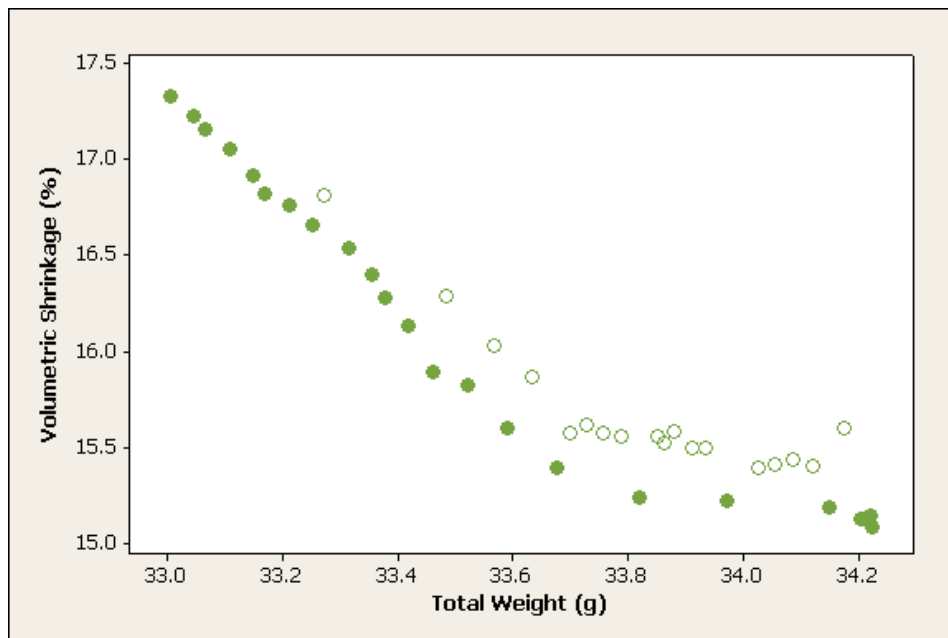


Figure 5.2-8. Graph with simulated values classified in efficient (full circles) and dominated values (empty circles).

Step 7: Multiple Criteria Process Window.

Figure 5.2-9 shows the efficient set classified in three areas, depending on the different level of compromise between PMs with the associated IM settings.

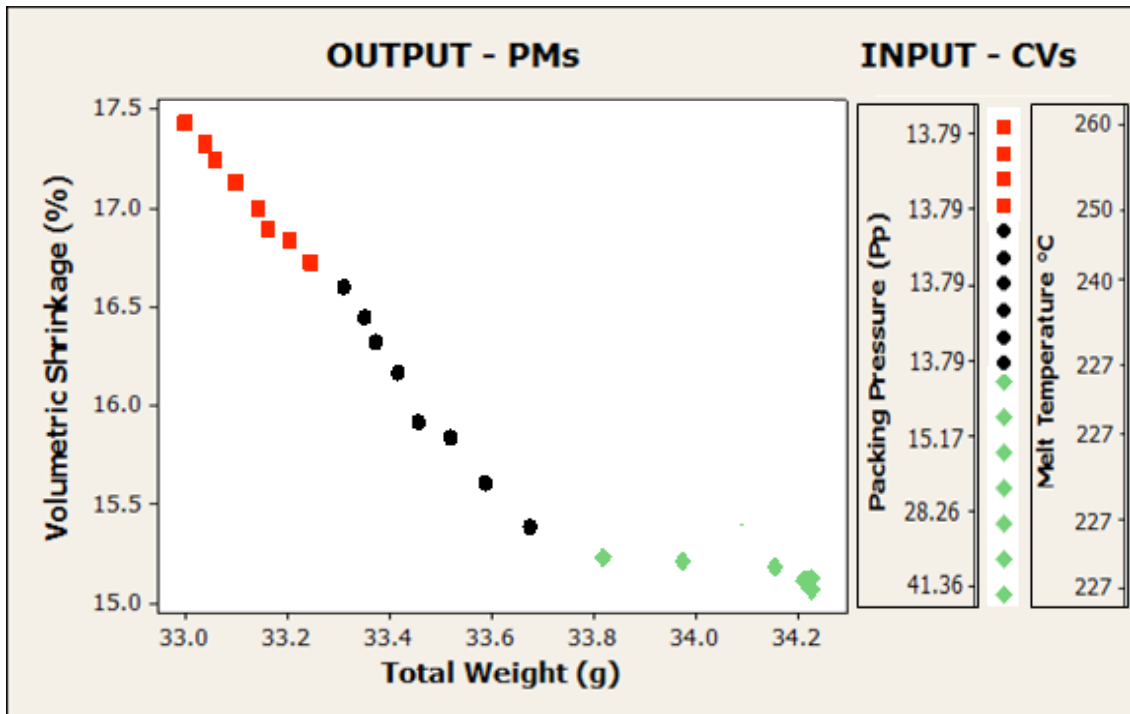


Figure 5.2-9. Multiple criteria process window classified in three areas for case 1.

5.2.1 Conclusion of case 1

The best compromises case 1 are found in two areas: (1) setting Melt Temperature at 227 °C and varying Packing pressure in the range of [13.79, 41.36] MPa and (2) setting Packing pressure in 13.79 MPa while varying Melt Temperature in the range of [227, 260] °C. The predicted values for the associated PMs are all within less than 10% error of the simulated values.

5.3 Case 2: Minimize Total Weight and Minimize Cycle Time

The PMs considered for the case 2 are Cycle Time (sec) and Total Weight (g). Cycle Time is important in economics terms and Total Weight is important for the quality of molded part. Both were to be minimized. The CVs are Melt Temperature and Mold Temperature. Both CVs were selected due their known effect on the PMs considered for the case. These are varied in the ranges [227, 260] °C and [13, 49] °C respectively. The chosen material was D21148 Lyondel Bassel Advanced Polyolefin USA Inc. Injection time was set at 1 sec, V/P Switch at 80%, packing time at 10sec, frozen at ejection set to 100%, and cooling time was set to be determined automatically. The results were obtained using Polymer Simulator Insight Moldflow software 2011. The application of the proposed method is described next.

Step 1: Perform an initial design of experiments.

A central composite design involving both variables and both PMs was carried out.

The initial results are shown in Table 5.3-1.

Table 5.3-1. Experimental design for Case 2

Run	Melt Temperature (°C)	Mold Temperature (°C)	Cycle Time (sec)	Total Weight (g)
1	227	13	202.8211	33.7279
2	227	31	255.3170	33.7064
3	227	49	408.5735	33.6704
4	244	13	207.8219	33.3848
5	244	31	260.5720	33.3582
6	244	49	412.8269	33.3288
7	260	13	212.5729	33.0336
8	260	31	265.3207	33.0075
9	260	49	415.5613	32.9792

The Figures 5.3-1 and 5.3-2 graphically shows that melt temperature have a larger effect on total weight than a cycle time: while mold temperature affects cycle time more. An increase in mold temperature results in a decrease in total weight but in an increase on cycle time. In the other hand, decreasing melt temperature decreases total weight.

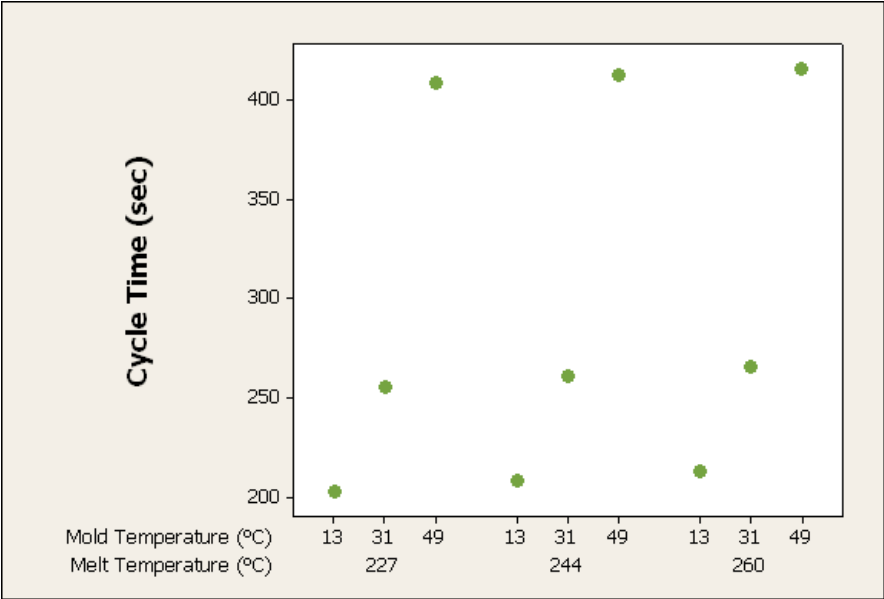


Figure 5.3-1. Graph of principal effect of CVs in Cycle Time for case 2.

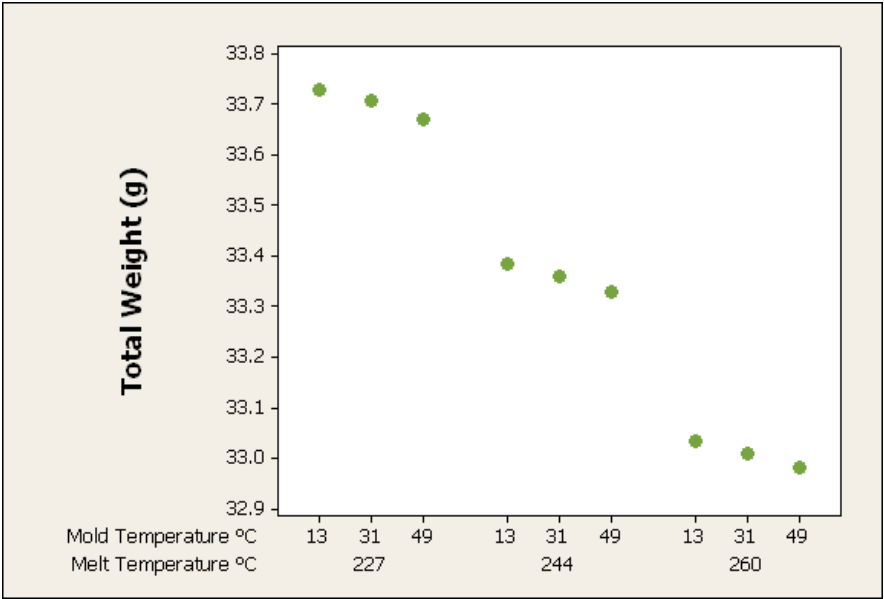


Figure 5.3-2. Graph of principal effect of CVs in Total Weight for case 2.

Step 2: Scale the controllable variables (CVs) and performance measures (PMs) to fall within -1 and 1.

As in the previous case each CV and PM must be between -1 and 1. This is accomplished through the usual method of using a linear transformation.

Step 3: Fit a Metamodel per PM.

The scaled data were used to generate second order regression metamodels. The ones corresponding to this case are shown next:

$$\begin{aligned} \text{Cycle Time} = & -0.4563 + 0.0419T_m + 0.9617T_w - 0.0036T_m^2 + 0.4665T_w^2 - \\ & 0.0065T_mT_w \end{aligned} \quad (5.2-1)$$

$$\text{R-Sq} = 100\%$$

$$\text{R-Sq (adj)} = 100\%$$

$$\begin{aligned} \text{Total Weight} = & 0.0157 - 0.9280T_m - 0.0748T_w - 0.0083T_m^2 - 0.0087T_w^2 + \\ & 0.0021T_mT_w \end{aligned} \quad (5.2-2)$$

$$\text{R-Sq} = 100\%$$

$$\text{R-Sq (adj)} = 99.99\%$$

Notice that both metamodels were above 90% in their R^2 values. The analysis of variance (ANOVA) of this case study is presented in Appendix 11.

Step 4: Use the metamodels to generate PMs Predictions in the experimental region of the CVs.

The previous second order regression metamodels and the 441 combinations of CVs shown in Figure 5.3-3 as a grid, were used to predict the values of the PMs and thus to find Predicted Feasible Region (PFR) in the space of the criteria shows in Figure 5.3-4.

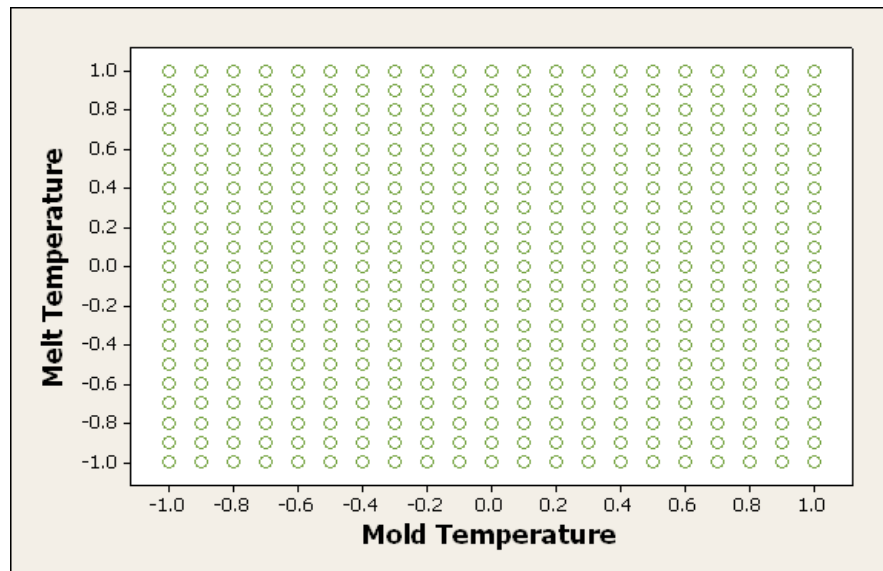


Figure 5.3-3. Experimental region of CVs for case 2.

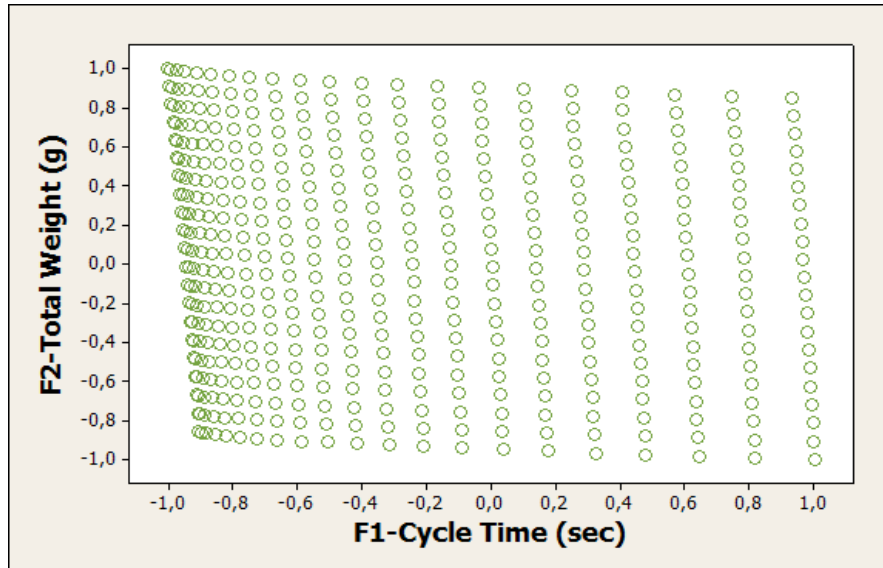


Figure 5.3-4. Predicted feasible region for case 2.

Step 5: Find the Efficient Frontier using the PMs' predictions.

In order to find the Predicted Efficient Solutions (PES) and their associated CVs' values definitions (1) and (2) were used. The pairwise comparisons were carried out using Excel. Figure 5.3-5 shows the predicted Non-Dominated set of solutions while Figure 5.3-6 shows the shape of the PFR and the location of PES.

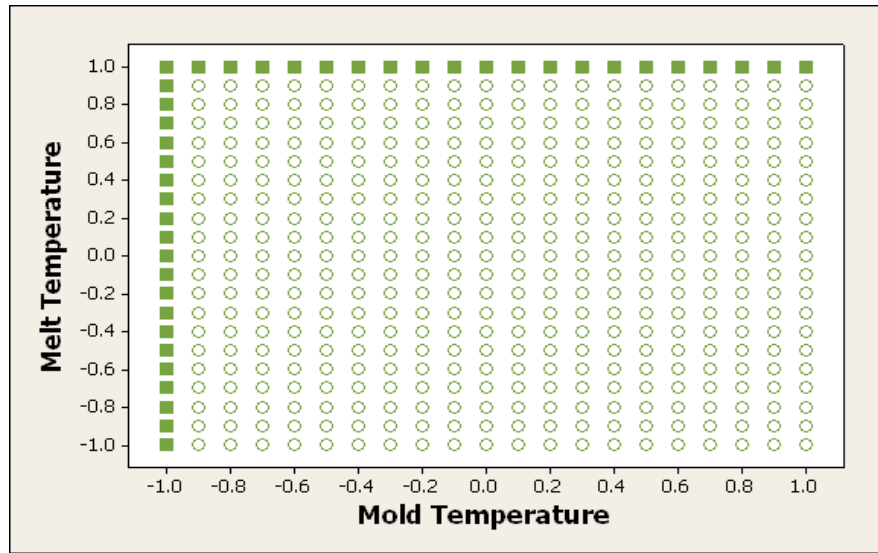


Figure 5.3-5. Predicted Non-Dominated (squares) and dominated set (empty circles) for case 2.

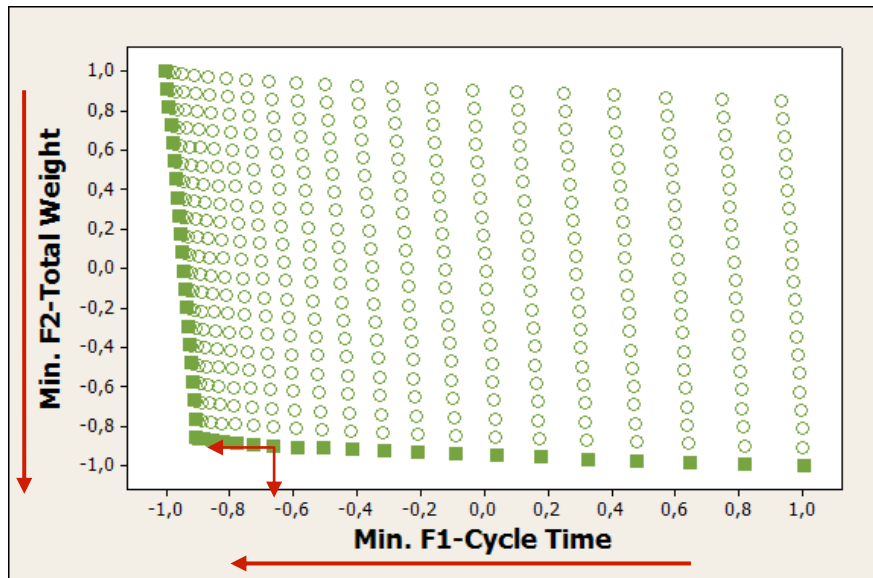


Figure 5.3-6. Predicted efficient set (squares) and dominates set (empty circles) for case 2.

Step 6: Validation.

All PES, were validated with the simulation software. These results are shown in Figure 5.3-7. The associated values of CVs, Predicted Solutions and simulation validations are shown in Table 8.2 Appendix A.

The results shows the good performance of the method, predicted runs, indeed, were never off by more than 5% of error. And all predicted solutions were indeed in the true efficient frontier.

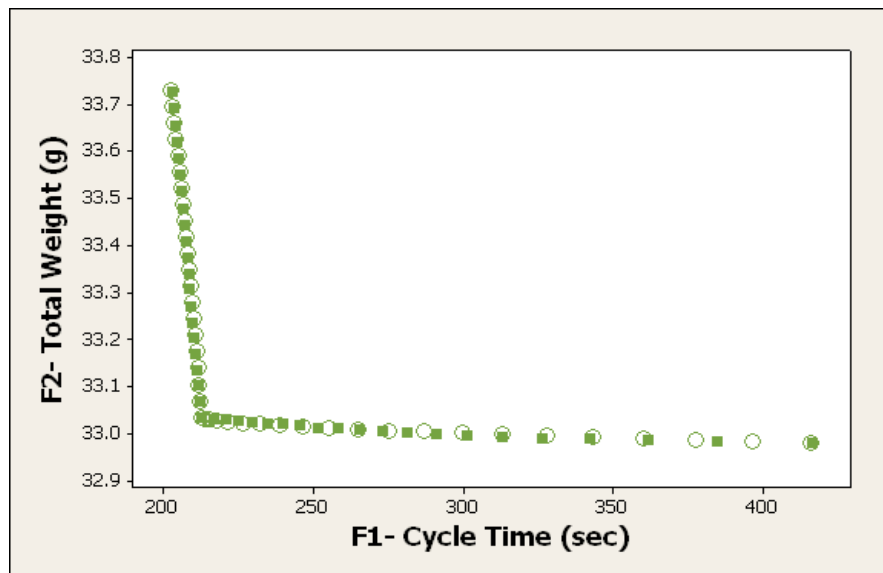


Figure 5.3-7. Predicted values (empty circles) vs. Simulation validation values (squares) for case 2.

Step 7: Multiple Criteria Process Window.

Figure 5.3-8 shows the efficient set classified in three areas, depending in the different level of compromise between PMs. The associated final process settings for case 2 are shown in this figure.

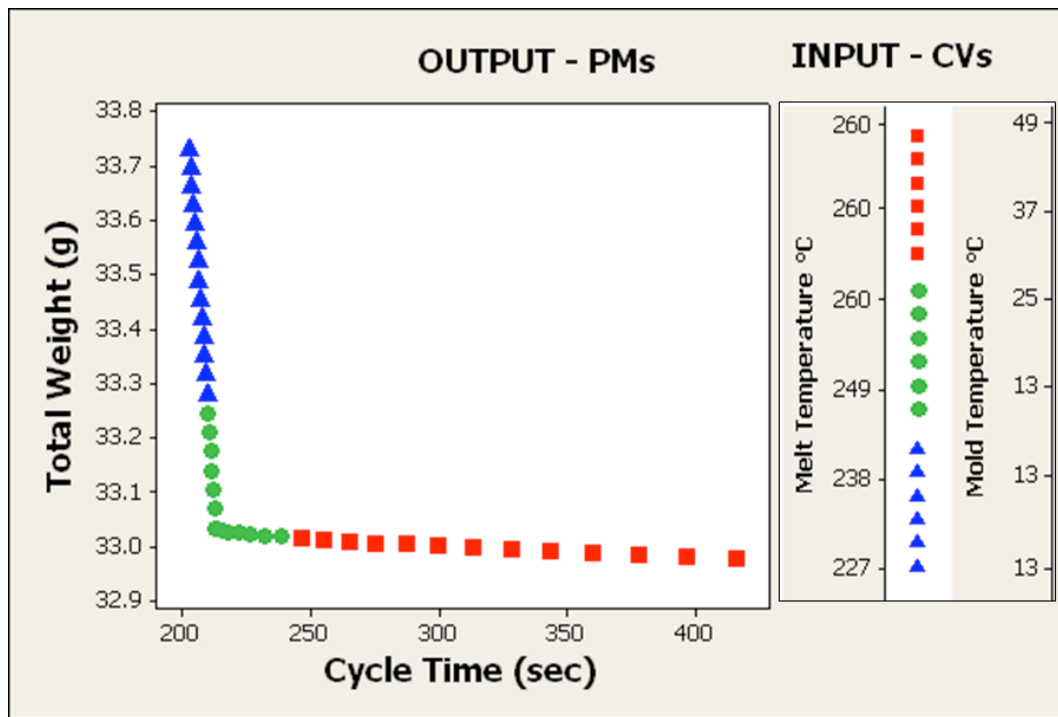


Figure 5.3-8. Multiple criteria process window classified in three areas for Case 2.

5.3.1 Conclusions for case 2

The best compromises case 2 are found in two areas: (1) setting Mold Temperature at 13 °C and varying Melt Temperature in the range of [227, 260] °C and (2) setting Melt Temperature in 260 °C while varying Mold Temperature in the range of [13, 49] °C. The predicted values for the associated PMs are all within less than 5% error of the simulated values.

5.4 Case 3: Minimize Total Weight, Minimize Volumetric shrinkage and Minimize Cycle Time

Case 3 considers the simultaneous optimization of three PMs. All of them must be minimized: Volumetric shrinkage (%), Total Weight (g) and Cycle Time (sec). Two CVs were selected: packing pressure and melt temperature. These are varied in the ranges [13.79, 41.36] MPa and [227, 260] °C. Experimental ranges for the CVs were determined using the recommended values from Moldflow 2011 material's database. The chosen material was: D21148 LyondelBassel Advanced Polyolefin USA Inc. The settings were: Mold temperature at 32°C, Injection time at 1 sec, V/P Switch-over at 80%, packing time at 10 sec and cooling time was set in automatic as in the previous case. The application of the proposed method is described next.

Step 1: Perform an initial design of experiments.

A central composite design involving both variables and both PMs was carried out.

The initial experimental design is shown in Table 5.4-1.

Table 5.4-1. Experimental design for case 3.

Run	Melt temperature (°C)	Packing pressure (Mpa)	Total Weight (g)	Volumetric Shrinkage (%)	Cycle Time (sec)
1	227	13.79	33.6978	15.64	254.3238
2	227	27.58	33.9739	15.24	254.3238
3	227	41.36	34.2130	15.11	254.3238
4	243	13.79	33.3561	16.31	259.5714
5	243	27.58	33.6953	16.16	259.5714
6	243	41.36	33.9110	15.99	259.5714
7	260	13.79	33.0058	17.34	264.3239
8	260	27.58	33.3910	17.21	264.3239
9	260	41.36	33.6307	16.91	264.3239

The Figures 5.4-1, 5.4-2 and 5.4-3 graphically show that the melt temperature has a good effect on total weigh a negative effect on volumetric shrinkage and cycle time. An increase in melt temperature results in a decrease on total weight but in an increase on volumetric shrinkage and cycle time. In the other hand, an increase in packing pressure results in an increase on total weight while in a decrease on volumetric shrinkage and apparently has no effect on cycle time.

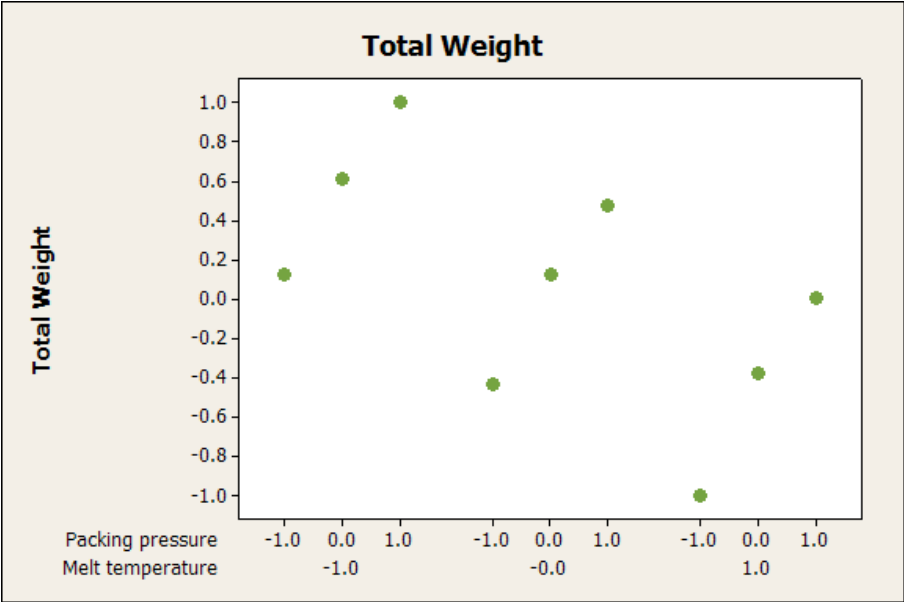


Figure 5.4-1. Graph of principal effect of CVs in Total weight for case 3.

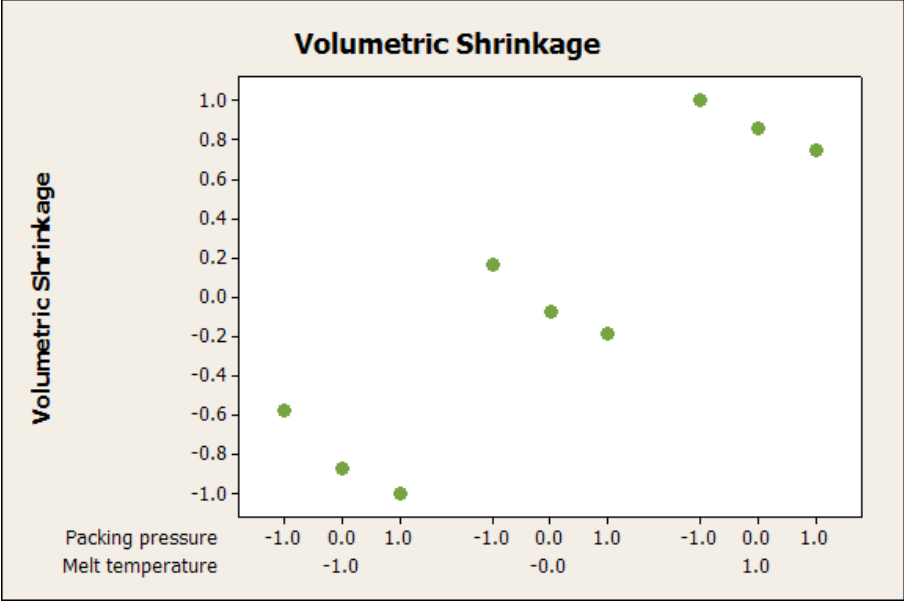


Figure 5.4-2. Graph of principal effect of CVs in Volumetric shrinkage for case 3.

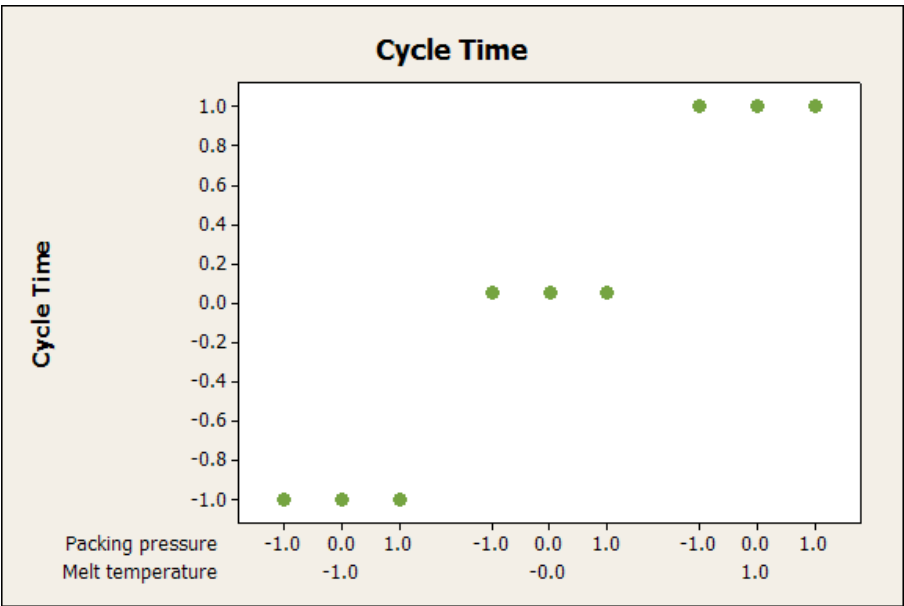


Figure 5.4-3. Graph of principal effect of CVs in Cycle time for case 3.

Step 2: Scale the controllable variables (CVs) and performance measures (PMs) to fall within -1 and 1.

Each CV and PM was scaled to fall within -1 and 1.

Step 3: Fit a Metamodel per PM.

The scaled data were used to generate the following second order regression metamodels:

$$\begin{aligned} \text{Total Weight} = & 0.1147 - 0.5128Pp + 0.4685Tm + 0.0121Pp^2 - 0.0843Tm^2 \\ & + 0.0456PpTm \end{aligned} \quad (5.3-1)$$

$$\text{R-Sq} = 99.89\%$$

$$\text{R-Sq (adj)} = 99.71\%$$

$$\begin{aligned} \text{Volumetric shrinkage} = & -0.0475 + 0.8176Pp - 0.1911Tm + 0.0545Pp^2 + 0.0119Tm^2 \\ & + 0.0217PpTm \end{aligned} \quad (5.3-2)$$

$$\text{R-Sq} = 99.52\%$$

$$\text{R-Sq (adj)} = 98.72\%$$

$$\begin{aligned} \text{Cycle Time} = & 0.0799 + 1.0000Pp + 0.0000Tm - 0.0799Pp^2 + 0.0000Tm^2 \\ & + 0.0000PpTm \end{aligned} \quad (5.3-3)$$

$$\text{R-Sq} = 100.00\%$$

$$\text{R-Sq(adj)} = 100.00\%$$

where T_m is Melt Temperature and P_p is Packing Pressure. All metamodells achieved R^2 values of more than 90%. The analysis of variance (ANOVA) of this case study is presented in Appendix 12.

Step 4: Use the metamodells to generate PMs Predictions in the experimental region of the CVs.

The previous second order regression metamodells and the 441 combinations of CVs shown in Figure as a grid, were used to predict the values of the PMs and thus to find Predicted Feasible Region (PFR) in the space of the criteria shows in Figure 5.4-4.

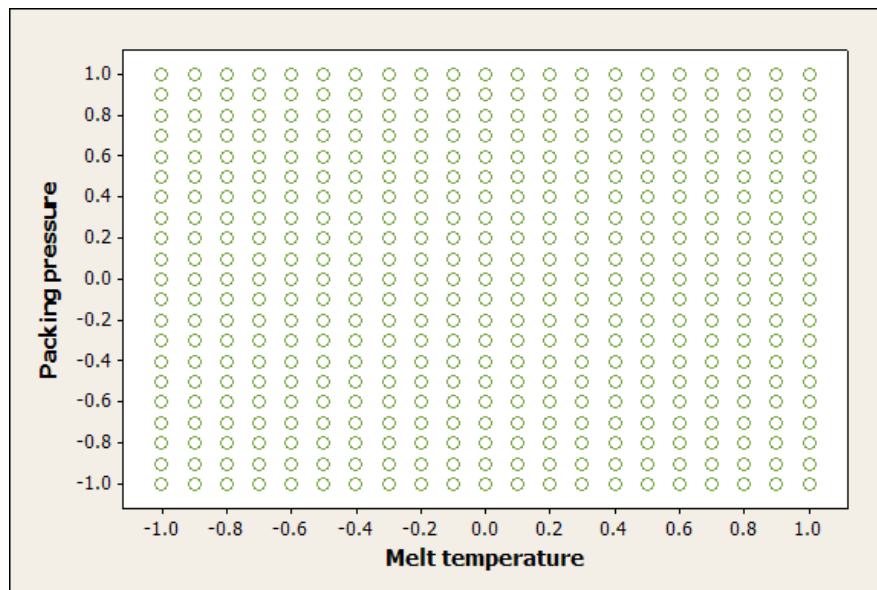


Figure 5.4-4. Experimental region of CVs for case 3.

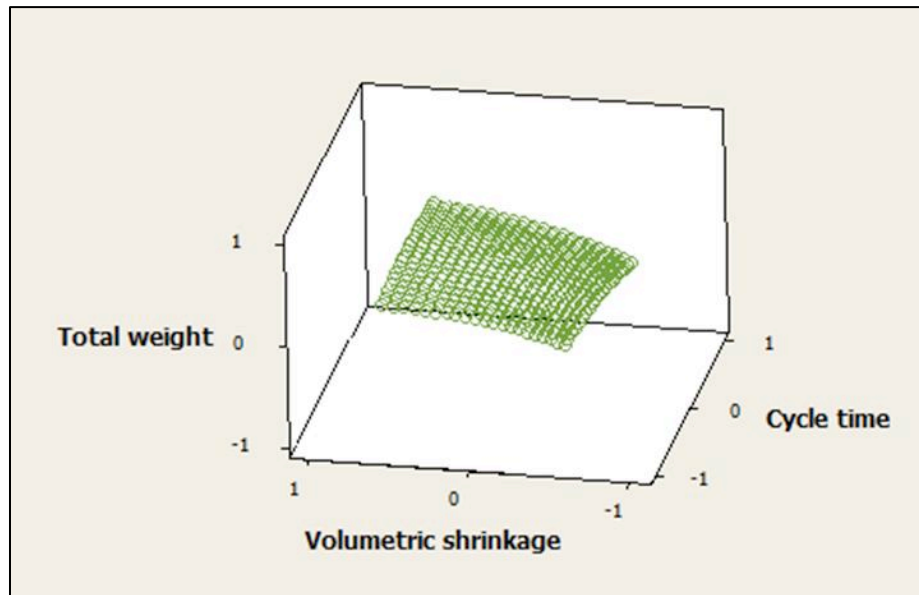


Figure 5.4-5. Predicted feasible region for case 3.

Step 5: Find the Efficient Frontier using the PMs' predictions.

In order to find the Predicted Efficient Solutions (PES) and their associated CVs' values definitions (1) and (2) were applied as before. Figure 5.4-6 shows the predicted Non-Dominated set of solutions while Figure 5.4-7 shows the shape of the PFR and the location of PES.

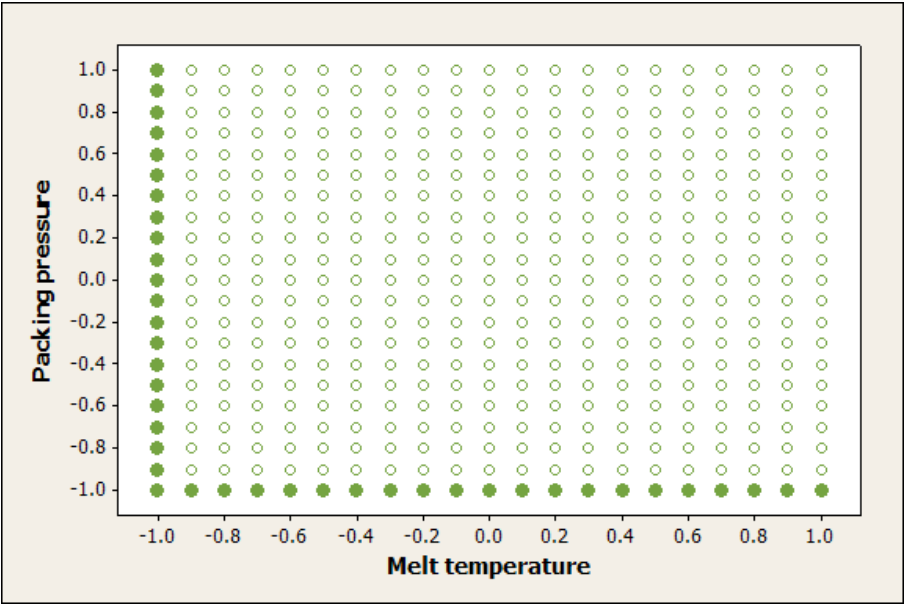


Figure 5.4-6. Predicted Non-Dominated set (full circles) and dominated set (empty circles) for case 3.

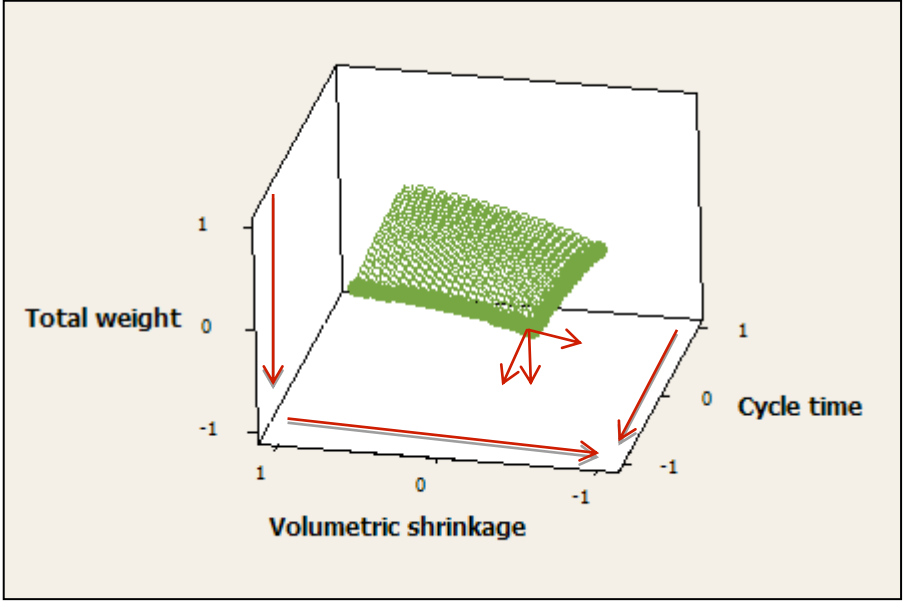


Figure 5.4-7. Predicted efficient set (full circles) and dominated set (empty circles) for case 3.

Step 6: Validation.

All PES, were validated with the simulation software. These results are shown in Figure 5.4-8. The associated values of CVs, Predicted Solutions and simulation validations are shown in Table 8.3 Appendix A.

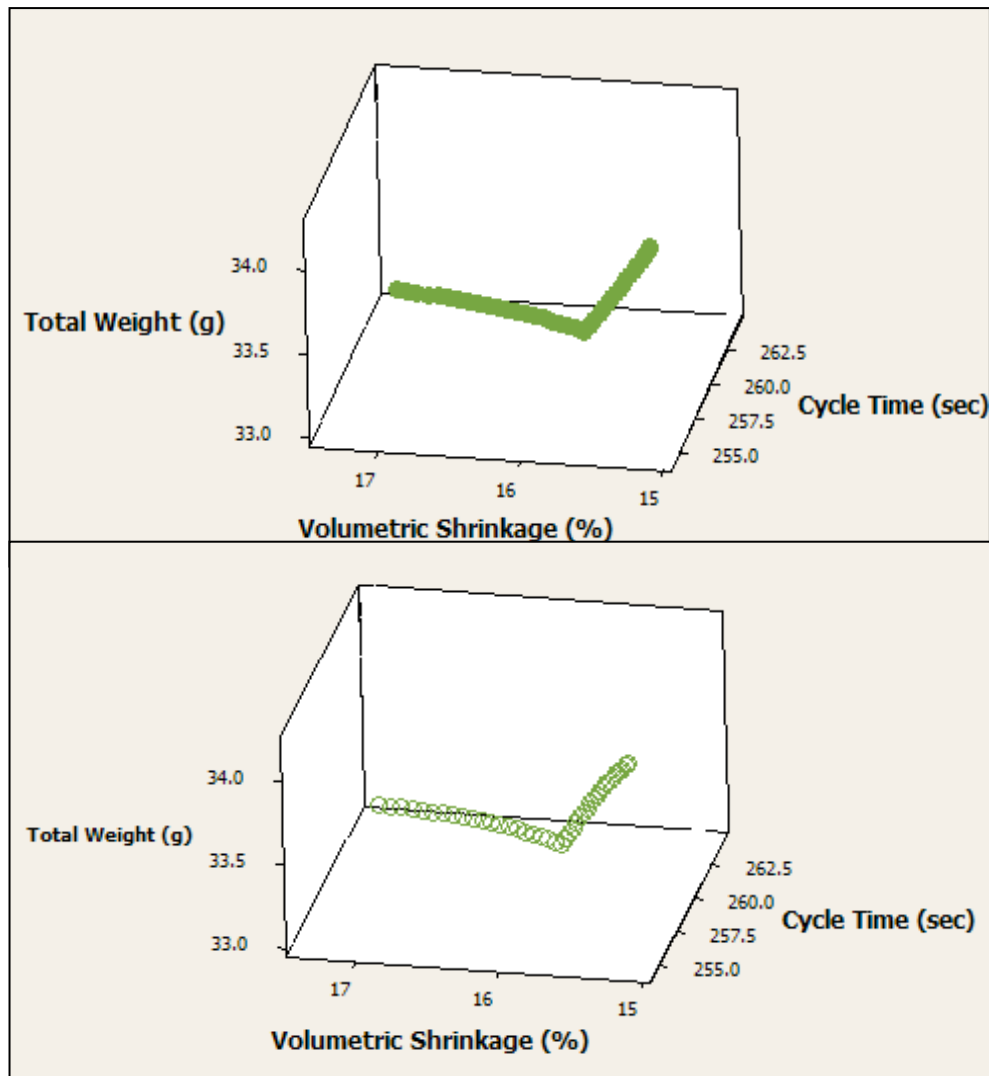


Figure 5.4-8. Predicted values (empty circles) vs. simulated values (full circles) for case 3.

The results of this case also show that the proposed method is effective to predict the EF. The approximation in this case is within less than 1 % of error. And all predicted solutions were indeed in the true efficient frontier.

Step 7: Multiple Criteria Process Window.

Figure shows the efficient set classified in three areas, depending in the different level of compromise between PMs. The associated final process settings for case 3 are shown in this figure.

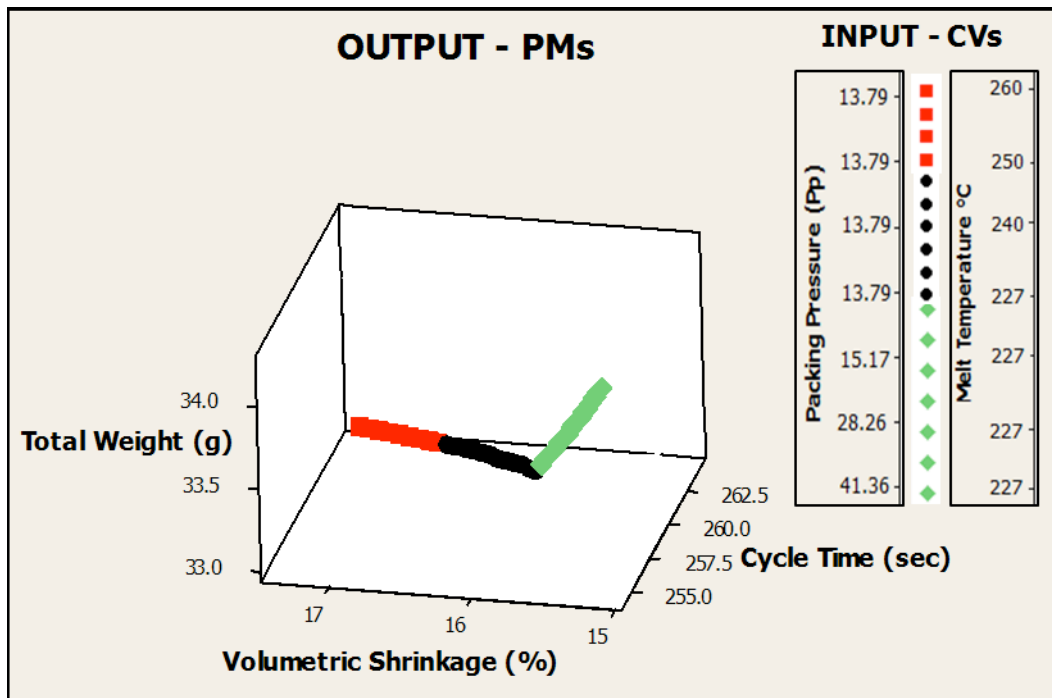


Figure 5.4-9. Multiple criteria process window classified in three areas for Case 3.

5.4.1 Conclusions of case 3

The best compromises for case 3 are found in two areas: (1) setting Melt Temperature at 227 °C and varying Packing pressure in the range of [13.79, 41.36] MPa and (2) setting Packing pressure in 13.79 MPa while varying Melt Temperature in the range of [227, 260] °C. The predicted values for the associated PMs are all within less than 1% error of the simulated values.

5.5 Comparison of the proposed method versus data envelopment analysis

As discussed in the literature review section of this thesis, there are many different methods to find the efficient frontier in IM problems. In our research group, Data Envelopment Analysis (DEA) has been used to solve multiple criteria optimization problems in polymer processes [9], [22], [33], [36], [41]. DEA has the advantage of finding efficient solutions through the use of a series of linear optimization problems, which is very computationally convenient. The efficient frontier identified through DEA, however, is often times constrained to convexity. If the true efficient frontier of a multiple criteria optimization problem is not convex, then several efficient solutions might escape detection through DEA as shown in the following comparison of efficient frontier, using the proposed method and DEA. The reader interested in

solving multiple criteria optimization problem using DEA can consult the previous works of our research group [46-47]. The results are shown in Figure 5.5-1.

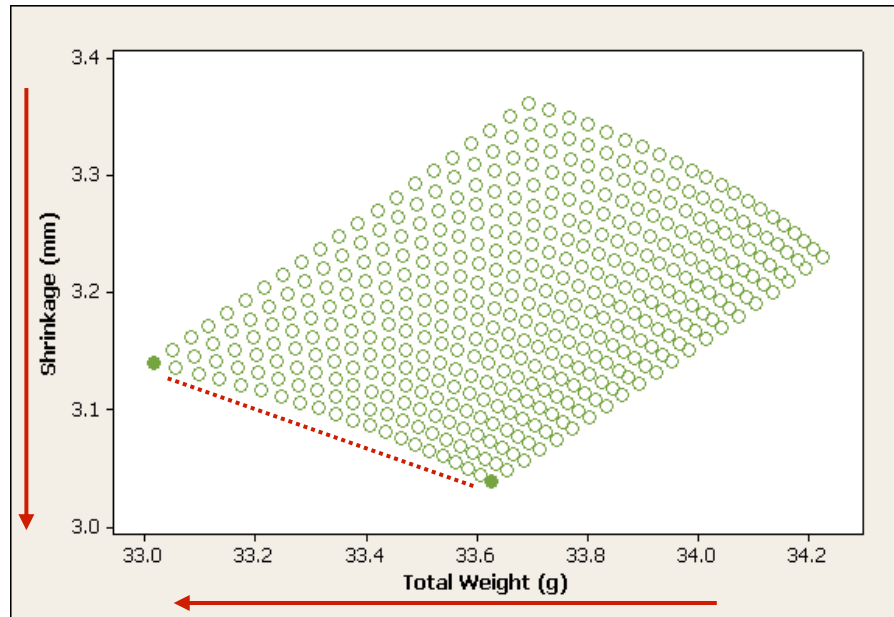


Figure 5.5-1. Efficient frontier using DEA solve.

Figure 5.5-1 illustrates the result with DEA. Only two efficient solutions are detected. Applying multiple criteria optimization concepts as shown in the proposed method, the completed characterization of EF is made, as it can be verified in Figure 5.5-2.

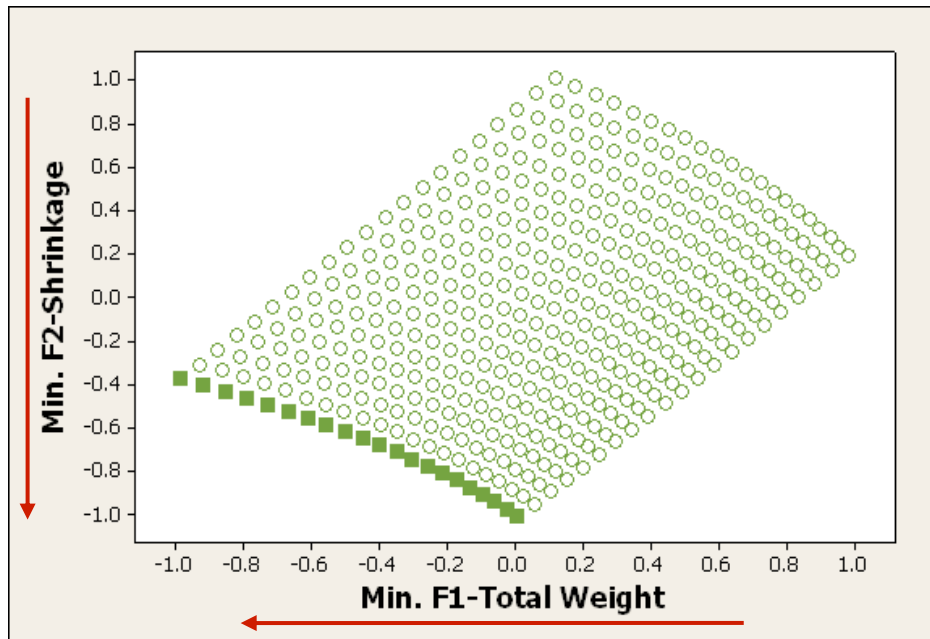


Figure 5.5-2. Efficient frontier using Proposed method.

From this comparison, an obvious combination of the strengths of both methods could be to use DEA to find the location of the efficient frontier with computational convenience to then finely characterize the efficient frontier through the use of the method proposed here. This integration will be pursued in our research group in the future.

6 CHAPTER

CONCLUSION AND FUTURE WORK

The performance of the strategy was demonstrated through three case studies.

In the first two cases, the optimization problem was defined considering two conflicting criteria and two controllable variables, while a third case involved three PMs and two controllable variables evidencing the capabilities of the strategy in finding the efficient frontiers.

The strategy is feasible, effective and efficient on prescribing competitive processing conditions in injection molding operations, and provides important information on the tradeoffs of quality criteria in conflict with a modest number of runs.

An experimental validation of the method is currently being undertaken at The Ohio State University. It is expected that these results follow the performance shown with simulations.

We are also currently working on improving the usability in the process window to make the method more applicable in the industry.

When compared to DEA, it is clear that the proposed strategy provides a better characterization of the efficient frontier, although at the cost of a larger computational burden mainly arising from requiring extensive pairwise comparisons. A strategy that combines the strength of DEA and the method proposed here will be developed in our group in the future.

Another idea that needs to be explored is the use of clustering techniques to make pairwise comparisons less numerous and therefore to provide the possibility to expand the application of the proposed method to several additional PMs.

Finally, a deeper look into how to transfer the concept of multiple criteria process window to the actual manufacturing site will be critical.

As a future work, we are also currently working on improving the usability in the process window to make the method more applicable in the industry in higher dimensionality.

Develop more industry-friendly process window. Then apply the methodology for more complicate problems such as:

System view for In-mold coating process

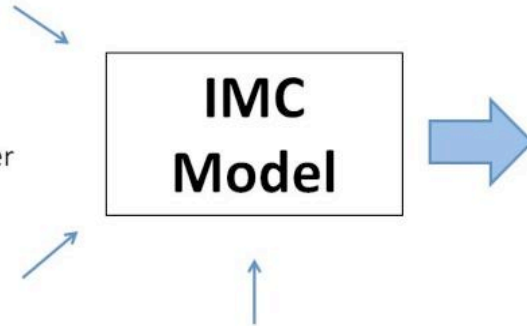
CPV

Materials:

Resin System
Initiator
Inhibitor
Promoter
Carbon black
Carbon Nanofiber
Nanoclay

Process:

T_{melt}
 T_{mold}
 P_{pack}
 t_{pack}
 t_j



PM

- Cycle time
- Shelf-life
- Injection pressure
- Clamping force
- Adhesion
- Abrasion resistance
- Conductivity
- Brittleness

Part

- IMC volume
- Flow length

7 REFERENCES

- [1] F. Yin, H. Mao, and L. Hua, "A hybrid of back propagation neural network and genetic algorithm for optimization of injection molding process parameters," *Materials & Design*, vol. 32, no. 6, pp. 3457-3464, Jun. 2011.
- [2] Wen-Chin Chen, Tung-Tsan Lai, Gong-Loung Fu, and Chen-Tai Chen, "A systematic optimization approach in the MISO Plastic Injection molding process," in *IEEE International Conference on Service Operations and Logistics, and Informatics, 2008. IEEE/SOLI 2008*, 2008, vol. 2, pp. 2741-2746.
- [3] W.-J. Deng, C.-T. Chen, C.-H. Sun, W.-C. Chen, and C.-P. Chen, "An effective approach for process parameter optimization in injection molding of plastic housing components," *Polymer - Plastics Technology and Engineering*, vol. 47, no. 9, pp. 910-919, 2008.
- [4] M.-S. Huang and T.-Y. Lin, "An innovative regression model-based searching method for setting the robust injection molding parameters," *Journal of Materials Processing Technology*, vol. 198, no. 1-3, pp. 436-444, Mar. 2008.
- [5] B. Ozcelik and T. Erzurumlu, "Comparison of the warpage optimization in the plastic injection molding using ANOVA, neural network model and genetic algorithm," *Journal of Materials Processing Technology*, vol. 171, no. 3, pp. 437-445, Feb. 2006.
- [6] T. Erzurumlu and B. Ozcelik, "Minimization of warpage and sink index in injection-molded thermoplastic parts using Taguchi optimization method," *Materials and Design*, vol. 27, no. 10, pp. 853-861, 2006.
- [7] W.-C. Chen, G.-L. Fu, P.-H. Tai, and W.-J. Deng, "Process parameter optimization for MIMO plastic injection molding via soft computing," *Expert Systems with Applications*, vol. 36, no. 2, Part 1, pp. 1114-1122, Mar. 2009.
- [8] A. Kramschuster, R. Cavitt, D. Ermer, Z. Chen, and L.-S. Turng, "Quantitative study of shrinkage and warpage behavior for microcellular and conventional injection molding," *Polymer Engineering and Science*, vol. 45, no. 10, pp. 1408-1418, 2005.
- [9] V. G. Loera, J. M. Castro, J. M. Diaz, O. L. . Mondragon, and M. Cabrera-Rios, "Setting the Processing Parameters in Injection Molding Through Multiple-Criteria Optimization: A Case Study," *IEEE Transactions on Systems, Man, and Cybernetics, Part C: Applications and Reviews*, vol. 38, no. 5, pp. 710-715, Sep. 2008.
- [10] C.-P. Chen, M.-T. Chuang, Y.-H. Hsiao, Y.-K. Yang, and C.-H. Tsai, "Simulation and experimental study in determining injection molding process parameters for thin-shell plastic parts via design of experiments analysis," *Expert Systems with Applications*, vol. 36, no. 7, pp. 10752-10759, Sep. 2009.
- [11] M.-S. Huang and T.-Y. Lin, "Simulation of a regression-model and PCA based searching method developed for setting the robust injection molding parameters of multi-quality characteristics," *International Journal of Heat and Mass Transfer*, vol. 51, no. 25-26, pp. 5828-5837, Dec. 2008.
- [12] J.-W. Chen, L. He, and B.-P. Xu, "The application of cavity pressure profile in the injection molding process parameters optimization," in *2010 International Conference*

- on Mechanic Automation and Control Engineering, MACE2010, June 26, 2010 - June 28, 2010*, Wuhan, China, 2010, pp. 5350-5353.
- [13] Wen-Chin Chen, Tung-Tsan Lai, Gong-Loung Fu, and Chen-Tai Chen, "A systematic optimization approach in the MISO Plastic Injection molding process," in *IEEE International Conference on Service Operations and Logistics, and Informatics, 2008. IEEE/SOLI 2008*, 2008, vol. 2, pp. 2741-2746.
- [14] G. Pötsch and W. Michaeli, *Injection molding: an introduction*. Hanser Verlag, 2008.
- [15] D. M. Bryce, *Plastic injection molding: manufacturing process fundamentals*. SME, 1996.
- [16] Wen-Chin Chen, Tung-Tsan Lai, Gong-Loung Fu, and Chen-Tai Chen, "A systematic optimization approach in the MISO Plastic Injection molding process," 2008, pp. 2741-2746.
- [17] C.-F. J. Kuo and T.-L. Su, "Optimization of injection molding processing parameters for LCD light-guide plates," *Journal of Materials Engineering and Performance*, vol. 16, no. 5, pp. 539-548, 2007.
- [18] W.-C. Chen, G.-L. Fu, P.-H. Tai, and W.-J. Deng, "Process parameter optimization for MIMO plastic injection molding via soft computing," *Expert Systems with Applications*, vol. 36, no. 2 PART 1, pp. 1114-1122, 2009.
- [19] D. Li, H. Zhou, P. Zhao, and Y. Li, "A Real-time process optimization system for injection molding," *Polymer Engineering and Science*, vol. 49, no. 10, pp. 2031-2040, 2009.
- [20] K.-C. Chang, Y. Hioe, M. G. Villarreal, and J. M. Castro, "Minimum 'Safe cycle time': Selecting the frozen layer thickness," *Polymer Engineering and Science*, vol. 49, no. 12, pp. 2320-2328, 2009.
- [21] D. Mathivanan and N. S. Parthasarathy, "Prediction of sink depths using nonlinear modeling of injection molding variables," *The International Journal of Advanced Manufacturing Technology*, vol. 43, pp. 654-663, Sep. 2008.
- [22] M. A. Urbano, M. G. Villarreal-Marroquín, J. M. Castro, M. S. Peña, and M. C. Rios, "Setting Process Conditions under Multiple Criteria." [Online]. Available: <http://www.highbeam.com/doc/1P3-1848735301.html>. [Accessed: 26-Nov-2011].
- [23] C. Fernandes, A. J. Pontes, J. C. Viana, and A. Gaspar-Cunha, "Using multiobjective evolutionary algorithms in the optimization of operating conditions of polymer injection molding," *Polymer Engineering and Science*, vol. 50, no. 8, pp. 1667-1678, 2010.
- [24] D. C. Montgomery, *Design and analysis of experiments*. John Wiley and Sons, 2008.
- [25] A. Kramschuster, R. Cavitt, D. Ermer, Z. Chen, and L.-S. Turng, "Quantitative study of shrinkage and warpage behavior for microcellular and conventional injection molding," *Polymer Engineering and Science*, vol. 45, no. 10, pp. 1408-1418, 2005.
- [26] Z. X. Zheng, Y. B. Wu, W. Xia, and W. P. Chen, "Process Optimization of Mid-Density Tungsten Alloy for Injection Process in Metal Injection Molding Based on Numerical Simulation," *Materials Science Forum*, vol. 628-629, pp. 599-604, Aug. 2009.

- [27] A. Santilli, I. Puente, and M. Tanco, "A factorial design study to determine the significant parameters of fresh concrete lateral pressure and initial rate of pressure decay," *Construction and Building Materials*, vol. 25, no. 4, pp. 1946-1955, 2011.
- [28] I. S. Kim, K. J. Son, Y. S. Yang, and P. K. D. V. Yaragada, "Sensitivity analysis for process parameters in GMA welding processes using a factorial design method," *International Journal of Machine Tools and Manufacture*, vol. 43, no. 8, pp. 763-769, Jun. 2003.
- [29] M. R. Barzegari and D. Rodrigue, "The effect of injection molding conditions on the morphology of polymer structural foams," in *Special Issue: POLYCHAR 16 Special Issue*, 111 River Street, Hoboken, NJ 07030-5774, United States, 2009, vol. 49, pp. 949-959.
- [30] R. Pantani, I. Coccorullo, V. Speranza, and G. Titomanlio, "Modeling of morphology evolution in the injection molding process of thermoplastic polymers," *Progress in Polymer Science*, vol. 30, no. 12, pp. 1185-1222, Dec. 2005.
- [31] Y. Gao and X. Wang, "Surrogate-based process optimization for reducing warpage in injection molding," *Journal of Materials Processing Technology*, vol. 209, no. 3, pp. 1302-1309, Feb. 2009.
- [32] K. Deb, *Multi-objective optimization using evolutionary algorithms*. John Wiley and Sons, 2001.
- [33] M. G. Villarreal-Marroquin, M. Cabrera-Rios, and J. M. Castro, "A multicriteria simulation optimization method for injection molding," *Journal of Polymer Engineering*, vol. 31, no. 5, pp. 397-407, 2011.
- [34] M. Ehrgott and K. Klamroth, "Connectedness of efficient solutions in multiple criteria combinatorial optimization," *European Journal of Operational Research*, vol. 97, no. 1, pp. 159-166, Feb. 1997.
- [35] J. Branke, T. Kauler, and H. Schmeck, "Guidance in evolutionary multi-objective optimization," *Advances in Engineering Software*, vol. 32, no. 6, pp. 499-507, 2001.
- [36] J. M. Castro, M. C. Ríos, and C. A. Mount-Campbell, "Modelling and simulation in reactive polymer processing," *Modelling and Simulation in Materials Science and Engineering*, vol. 12, p. S121-S149, May 2004.
- [37] I. Ferreira, O. De Weck, P. Saraiva, and J. Cabral, "Multidisciplinary optimization of injection molding systems," *Structural and Multidisciplinary Optimization*, vol. 41, no. 4, pp. 621-635, 2010.
- [38] J. Cheng, J.-R. Tan, and L.-L. Jin, "Multi-objective intelligent optimization of injection molding parameters based on BP-NSGA," *Jisuanji Jicheng Zhizao Xitong/Computer Integrated Manufacturing Systems, CIMS*, vol. 15, no. 10, pp. 1900-1906, 2009.
- [39] S. L. Faulkenberg and M. M. Wiecek, "On the quality of discrete representations in multiple objective programming," *Optimization and Engineering*, vol. 11, pp. 423-440, Dec. 2009.
- [40] H. R. Sayarshad and T. Marler, "A new multi-objective optimization formulation for rail-car fleet sizing problems," *Operational Research*, vol. 10, pp. 175-198, Oct. 2009.
- [41] Department of Industrial, Welding, and Systems Engineering, The Ohio State University, 210 Baker Systems, 1971 Neil Avenue, USA, C.-R. Mauricio, C. J. M, and

- M.-C. C. A, "Multiple quality criteria optimization in reactive in-mold coating with a data envelopment analysis approach II: A case with more than three performance measures," *Journal of polymer engineering*, vol. 24, no. 4, pp. 435-450, 2004.
- [42] V. Hessel, B. Cortese, and M. H. J. M. de Croon, "Novel process windows - Concept, proposition and evaluation methodology, and intensified superheated processing," *Chemical Engineering Science*, vol. 66, no. 7, pp. 1426-1448, 2011.
- [43] T. Erzurumlu and B. Ozcelik, "Minimization of warpage and sink index in injection-molded thermoplastic parts using Taguchi optimization method," *Materials and Design*, vol. 27, no. 10, pp. 853-861, 2006.
- [44] Data base Moldflow Insight 2011.
- [45] Mauricio Cabrera-Rios, Multiple Criteria Optimization Studies in Reactive In-Mold Coating: Coating: Polymer processing improvement through data envelopment analysis and nonlinear optimization, VDM Verlag DR Müller, 2009, ISBN-13: 978-3639212914.
- [46] Mauricio Cabrera-Rios, Multiple Criteria Optimization Studies in Reactive In-Mold Coating: Coating: Polymer processing improvement through data envelopment analysis and nonlinear optimization, VDM Verlag DR Müller, 2009, ISBN-13: 978-3639212914

8 APPENDIX A

This appendix contains all the data associated to the efficient solutions in all cases studies.

Table 8-1. Predicted efficient solutions and simulated efficient solutions of Case 1.

Run	Controllable variables		Predicted - Efficient Solutions		Validated - Efficient Solutions	
	Melt Temperature (°C)	Packing Pressure (MPa)	Total Weight (g)	Volumetric shrinkage (mm)	Total Weight (g)	Volumetric shrinkage (mm)
1	227	13.79	33.6932	15.56	33.6983	15.57
2	228	13.79	33.6588	15.64	33.6760	15.39
3	230	13.79	33.6244	15.72	33.6337	15.87
4	232	13.79	33.5901	15.80	33.5902	15.6
5	233	13.79	33.5558	15.88	33.5685	16.03
6	235	13.79	33.5216	15.96	33.5216	15.82
7	237	13.79	33.4875	16.04	33.4832	16.29
8	238	13.79	33.4534	16.13	33.4618	15.89
9	240	13.79	33.4194	16.22	33.4199	16.13
10	242	13.79	33.3854	16.30	33.3775	16.28
11	243	13.79	33.3515	16.39	33.3567	16.4
12	245	13.79	33.3176	16.48	33.3155	16.54
13	247	13.79	33.2838	16.57	33.2726	16.81
14	248	13.79	33.2500	16.66	33.2525	16.66
15	250	13.79	33.2163	16.76	33.2108	16.76
16	252	13.79	33.1827	16.85	33.1690	16.82
17	253	13.79	33.1491	16.95	33.1485	16.92
18	255	13.79	33.1156	17.05	33.1077	17.05
19	257	13.79	33.0821	17.15	33.0665	17.16
20	258	13.79	33.0487	17.25	33.0464	17.23
21	260	13.79	33.0153	17.35	33.0069	17.33

	Controllable variables		Predicted - Efficient Solutions		Validated - Efficient Solutions	
Run	Melt Temperature (°C)	Packing Pressure (MPa)	Total Weight (g)	Volumetric shrinkage (mm)	Total Weight (g)	Volumetric shrinkage (mm)
23	227	16.55	33.7664	15.49	33.7574	15.57
24	227	17.93	33.8013	15.46	33.7881	15.56
25	227	19.30	33.8351	15.43	33.8189	15.24
26	227	20.68	33.8678	15.40	33.8504	15.56
27	227	22.06	33.8994	15.37	33.8813	15.58
28	227	23.44	33.9298	15.34	33.9112	15.5
29	227	24.82	33.9592	15.31	33.8630	15.52
30	227	26.20	33.9875	15.29	33.9340	15.5
31	227	27.58	34.0146	15.26	33.9726	15.22
32	227	28.95	34.0406	15.24	34.0268	15.39
33	227	30.33	34.0656	15.22	34.0543	15.41
34	227	31.71	34.0894	15.20	34.0856	15.44
35	227	33.09	34.1121	15.18	34.1201	15.4
36	227	34.47	34.1337	15.16	34.1508	15.19
37	227	35.85	34.1542	15.14	34.1765	15.6
38	227	37.22	34.1736	15.13	34.2051	15.13
39	227	38.60	34.1919	15.11	34.2225	15.14
40	227	39.98	34.2090	15.10	34.2127	15.13
41	227	41.36	34.2251	15.09	34.2229	15.08

Table 8-2. Predicted efficient solutions and simulated efficient solutions of Case 2.

Run	Controllable variables		Predicted - Efficient Solutions		Validated - Efficient Solutions	
	Melt Temperature (°C)	Mold Temperature (°C)	Cycle Time (sec)	Total Weight (g)	Cycle Time (sec)	Total Weight (g)
1	227	13	202.4640	33.7292	202.8211	33.7279
2	229	13	203.0509	33.6950	203.327	33.6914
3	230	13	203.6302	33.6607	203.8236	33.6556
4	232	13	204.2019	33.6264	204.3212	33.62
5	234	13	204.7660	33.5920	204.8262	33.584
6	235	13	205.3225	33.5575	205.5661	33.5492
7	237	13	205.8715	33.5229	206.0727	33.5144
8	239	13	206.4128	33.4883	206.5703	33.479
9	240	13	206.9466	33.4537	207.0663	33.4444
10	242	13	207.4728	33.4190	207.5726	33.4089
11	244	13	207.9914	33.3842	208.0675	33.3747
12	245	13	208.5025	33.3493	208.3251	33.3401
13	247	13	209.0059	33.3144	208.8233	33.3059
14	248	13	209.5018	33.2794	209.3261	33.2705
15	250	13	209.9900	33.2444	209.8251	33.2363
16	252	13	210.4707	33.2093	210.3194	33.2023
17	253	13	210.9438	33.1741	210.8182	33.1681
18	255	13	211.4094	33.1389	211.3256	33.1344
19	257	13	211.8673	33.1036	211.8183	33.101
20	258	13	212.3177	33.0683	212.0735	33.067
21	260	13	212.7605	33.0329	212.5729	33.0336
22	260	15	213.4914	33.0308	216.5723	33.0312
23	260	17	215.2150	33.0286	220.8155	33.0285
24	260	18	217.9310	33.0264	225.0759	33.0266
25	260	20	221.6396	33.0241	229.8162	33.0232
26	260	22	226.3407	33.0217	234.8173	33.0208
27	260	24	232.0343	33.0193	240.0635	33.0192
28	260	26	238.7204	33.0168	245.569	33.0163
29	260	27	246.3991	33.0142	251.5715	33.0126
30	260	29	255.0703	33.0116	258.0772	33.0108

	Controllable variables		Predicted - Efficient Solutions		Validated - Efficient Solutions	
Run	Melt Temperature (°C)	Mold Temperature (°C)	Cycle Time (sec)	Total Weight (g)	Cycle Time (sec)	Total Weight (g)
31	260	31	264.7341	33.0089	265.3207	33.0075
32	260	33	275.3903	33.0062	273.0679	33.004
33	260	35	287.0391	33.0034	281.3291	33.0015
34	260	36	299.6804	33.0005	290.8255	32.9993
35	260	38	313.3143	32.9975	301.3164	32.9963
36	260	40	327.9406	32.9945	313.0744	32.9932
37	260	42	343.5595	32.9914	326.5683	32.9904
38	260	44	360.171	32.9883	342.3226	32.9875
39	260	45	377.7749	32.9851	361.5669	32.9848
40	260	47	396.3714	32.9818	385.0742	32.9821
41	260	49	415.9604	32.9785	416.5613	32.9792

Table 8-3. Predicted efficient solutions and simulated efficient solutions of Case 3.

Run	Predicted - Efficient Solutions			Validated - Efficient Solutions		
	Total Weight (g)	Volumetric shrinkage (mm)	Cycle time (sec)	Total Weight (g)	Volumetric shrinkage (mm)	Cycle time (sec)
1	33.6893	15.57	254.3238	33.6931	15.56	254.3239
2	33.6542	15.65	254.8997	33.6568	15.64	254.8999
3	33.6193	15.73	255.4676	33.6208	15.73	255.4679
4	33.5845	15.81	256.0275	33.5850	15.81	256.0279
5	33.5498	15.89	256.5795	33.5495	15.90	256.5799
6	33.5153	15.97	257.1234	33.5142	15.98	257.1240
7	33.4809	16.05	257.6594	33.4792	16.07	257.6600
8	33.4467	16.14	258.1873	33.4444	16.15	258.1882
9	33.4127	16.22	258.7073	33.4099	16.24	258.7083
10	33.3787	16.31	259.2193	33.3756	16.33	259.2204
11	33.3450	16.40	259.7233	33.3416	16.42	259.7246
12	33.3113	16.49	260.2193	33.3078	16.51	260.2208
13	33.2779	16.58	260.7073	33.2743	16.60	260.7090
14	33.2445	16.67	261.1873	33.2410	16.69	261.1893
15	33.2113	16.76	261.6594	33.2080	16.78	261.6616
16	33.1783	16.86	262.1235	33.1752	16.87	262.1259
17	33.1454	16.95	262.5795	33.1427	16.97	262.5822
18	33.1126	17.05	263.0276	33.1104	17.06	263.0305
19	33.0800	17.15	263.4677	33.0783	17.16	263.4709
20	33.0475	17.25	263.8998	33.0466	17.25	263.9033
21	33.0152	17.35	264.3239	33.0150	17.35	264.3277
22	33.7245	15.55	254.3238	33.7302	15.53	254.3239
23	33.7587	15.52	254.3238	33.7662	15.49	254.3239
24	33.7918	15.49	254.3238	33.8011	15.46	254.3238
25	33.8240	15.47	254.3238	33.8349	15.43	254.3238
26	33.8551	15.44	254.3238	33.8676	15.40	254.3238
27	33.8852	15.42	254.3238	33.8992	15.37	254.3238
28	33.9143	15.39	254.3238	33.9297	15.34	254.3238
29	33.9424	15.37	254.3238	33.9591	15.31	254.3239
30	33.9694	15.35	254.3238	33.9873	15.29	254.3239

	Predicted - Efficient Solutions			Validated - Efficient Solutions		
Run	Total Weight (g)	Volumetric shrinkage (mm)	Cycle time (sec)	Total Weight (g)	Volumetric shrinkage (mm)	Cycle time (sec)
31	33.9955	15.32	254.3238	34.0145	15.26	254.3239
32	34.0205	15.30	254.3238	34.0405	15.24	254.3240
33	34.0445	15.27	254.3238	34.0655	15.22	254.3240
34	34.0675	15.25	254.3238	34.0893	15.20	254.3241
35	34.0894	15.23	254.3238	34.1121	15.18	254.3242
36	34.1104	15.21	254.3238	34.1337	15.16	254.3242
37	34.1303	15.18	254.3238	34.1542	15.14	254.3243
38	34.1492	15.16	254.3238	34.1736	15.13	254.3244
39	34.1671	15.14	254.3238	34.1919	15.11	254.3245
40	34.1840	15.12	254.3238	34.2091	15.10	254.3246
41	34.1999	15.10	254.3238	34.2252	15.09	254.3247

Table 8-4. Predicted efficient settings for Case 3.

Run	Controllable variables	
	Melt Temperature (°C)	Packing Pressure (MPa)
1	227	13.79
2	228.65	13.79
3	230.3	13.79
4	231.95	13.79
5	233.6	13.79
6	235.25	13.79
7	236.9	13.79
8	238.55	13.79
9	240.2	13.79
10	241.85	13.79
11	243.5	13.79
12	245.15	13.79
13	246.8	13.79
14	248.45	13.79
15	250.1	13.79
16	251.75	13.79
17	253.4	13.79
18	255.05	13.79
19	256.7	13.79
20	258.35	13.79
21	260	13.79
22	227	15.1685
23	227	16.547
24	227	17.9255
25	227	19.304
26	227	20.6825

	Controllable variables	
Run	Melt Temperature (°C)	Packing Pressure (MPa)
27	227	22.061
28	227	23.4395
29	227	24.818
30	227	26.1965
31	227	27.575
32	227	28.9535
33	227	30.332
34	227	31.7105
35	227	33.089
36	227	34.4675
37	227	35.846
38	227	37.2245
39	227	38.603
40	227	39.9815
41	227	41.36

9 APPENDIX B

In this appendix, a way of validation of the proposed method is presented. Through two case studies the methodology to generate multiple criteria process windows is validated. These cases are studied and presented in a previous chapter. The way to validate the results obtained is classified in 4 areas the CV's to confirm if after the application of the proposed method the efficient frontier and the associated values of CVs are in the same expected area.

First we have to identify the 4 areas of CVs. After that, make a graph with CVs classification as well the feasible region. As that way, we map-out the values of CVs that are in the efficient frontier. If the dominate values of CVs map-out to the same efficient frontier area, the validation indicate that the method to identified the EF is effective and efficient.

9.1 Case A

The case 1: Minimize Shrinkage and Minimize Total Weight, presented in the section 5.1, is now validated using a method of classification. For this purpose here present the CVs classified

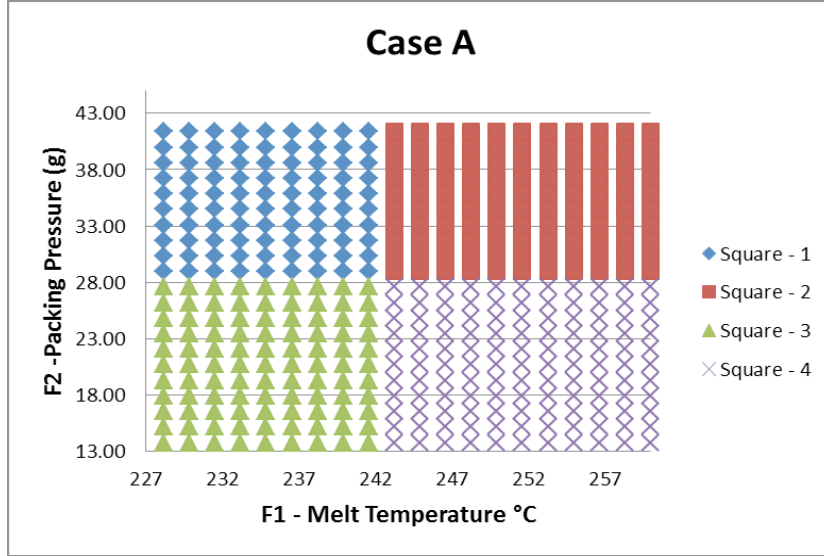


Figure 9.1-1. CVs classification by 4 position groups.

For this aim, the grid of combination of CV's is classified in 4 areas. After the application of the method, the efficient frontier is found as well the associated values of CVs and is shown in the follow Figure 9.1-2 and Figure 9.1-3 respectively.

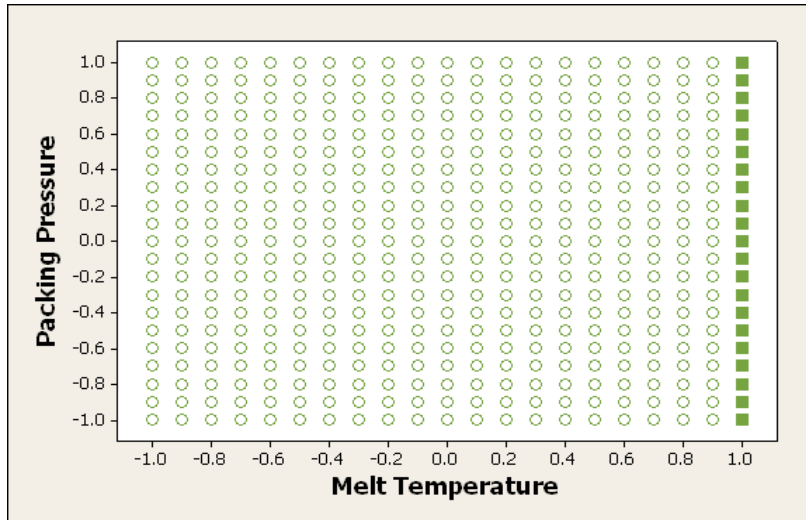


Figure 9.1-2. Dominate CVs after applied the proposed method.

Figure above shows the dominate set of CVs are found setting the Melt Temperature in the high values. Base on previous classification the values of CVs are in the square 2 and 4. In addition we expect that the efficient frontier have to be in the same squares.

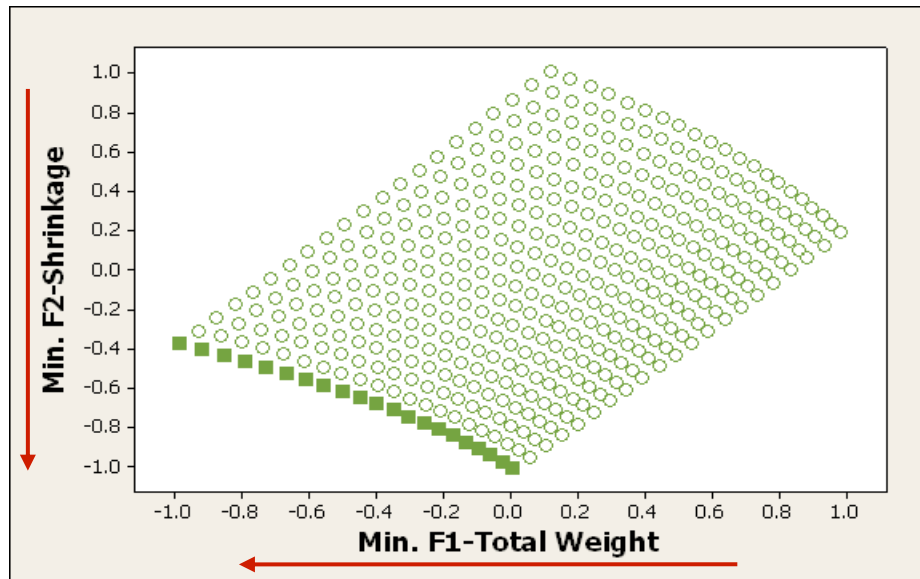


Figure 9.1-3. Efficient frontier after applied the proposed method.

Figure 9.1-4 shown the EF classified in base in the first classification of CVs. According to the first classification, in the previous Figures the dominate area is in the square 2 and 4. Now we expect that the EF is in the same squares.

In addition, when the total of combination is high, the classification or clustering will be an option. For this case if we only want to work with the square 2 and 4 we can obtain the result using less number of predictions.

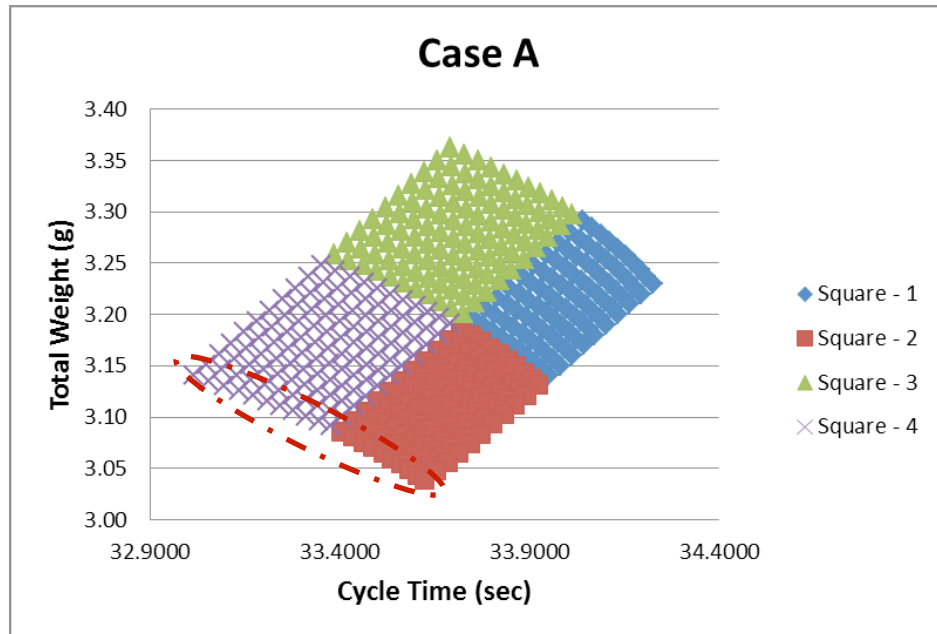


Figure 9.1-4. Efficient frontier classified in 4 areas.

9.2 Case B

The case 2: Minimize Total Weight and Cycle Time, presented in the section 5.2, is now evaluated using the same method for validation.

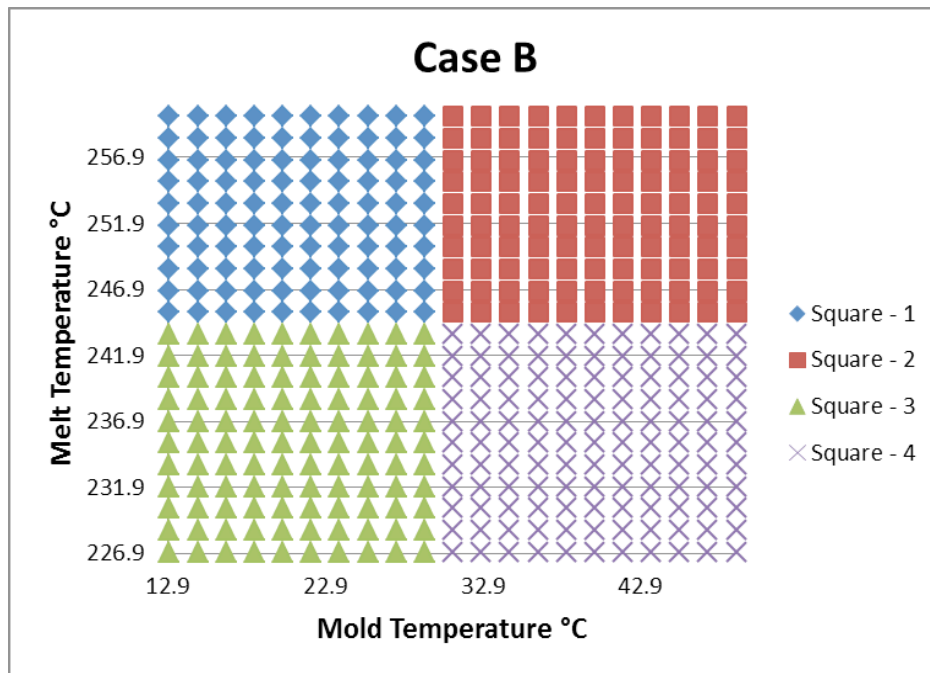


Figure 9.2-1. . CVs classification by 4 position groups.

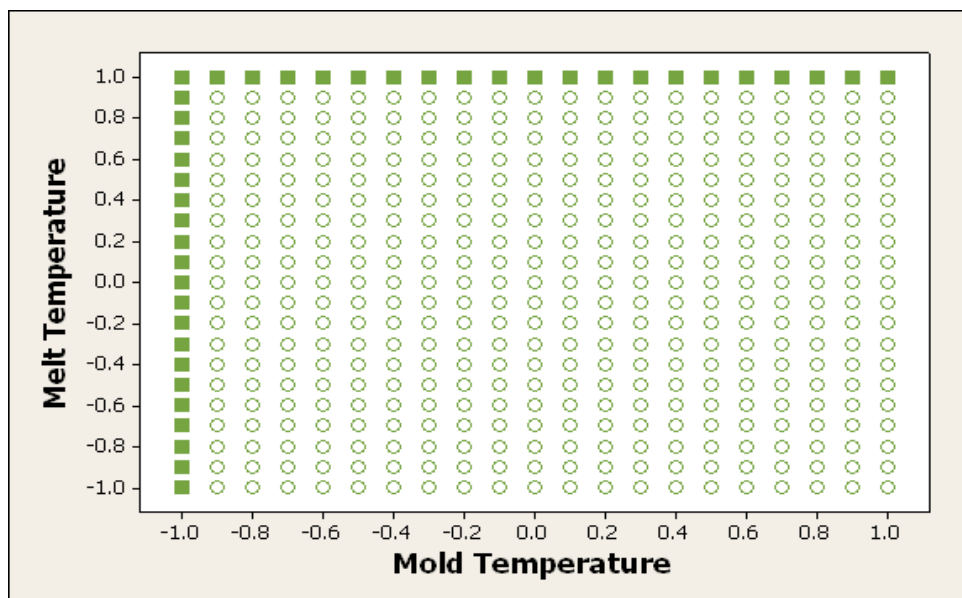


Figure 9.2-2. Dominate CVs after applied the proposed method case 2.

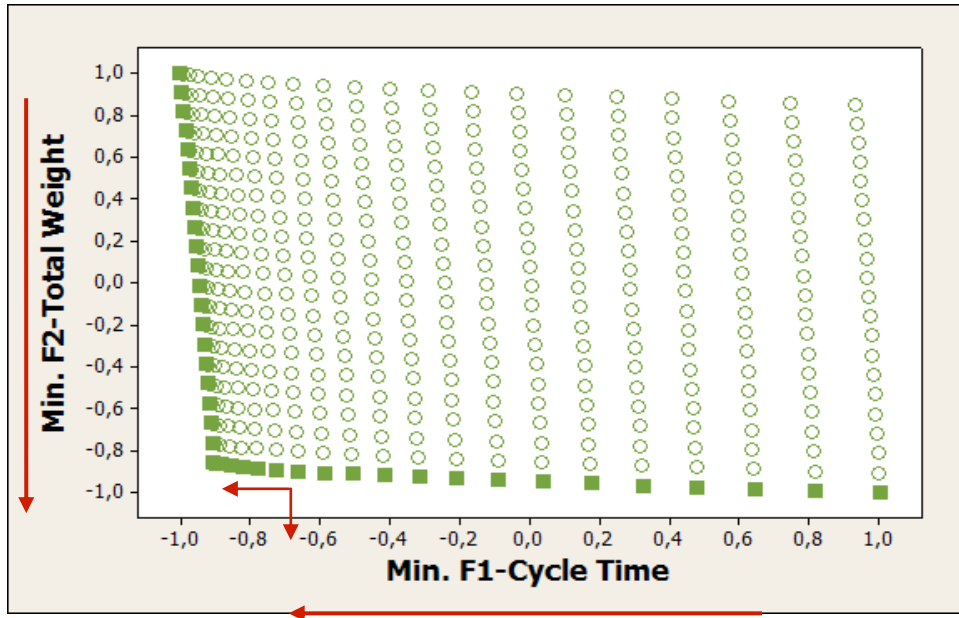


Figure 9.2-3. Efficient frontier after applied the proposed method case 2.

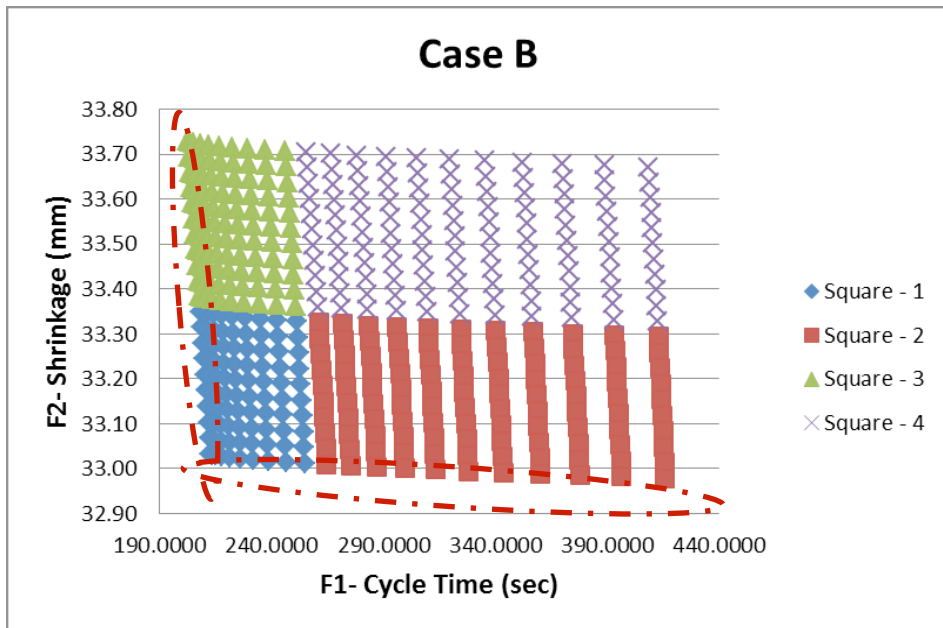
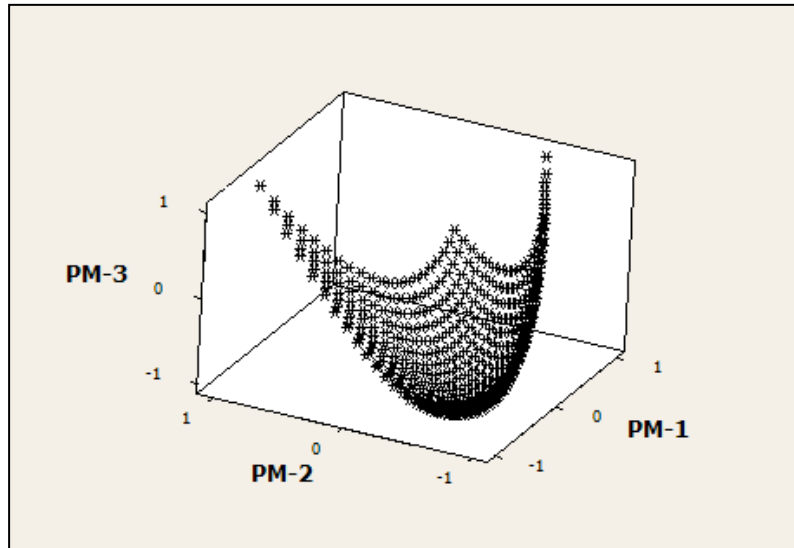


Figure 9.2-4. Efficient frontier classified in 4 areas.

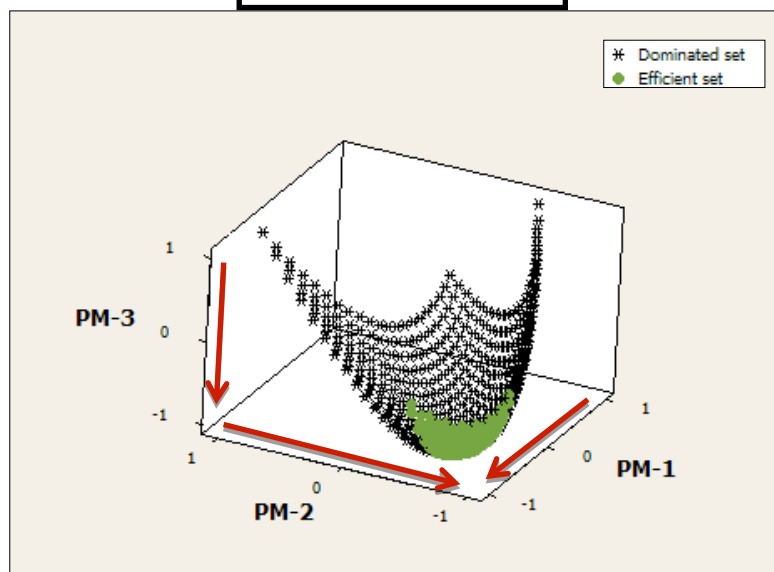
10 APPENDIX D

This appendix shows different optimization cases considering simultaneously three criteria.

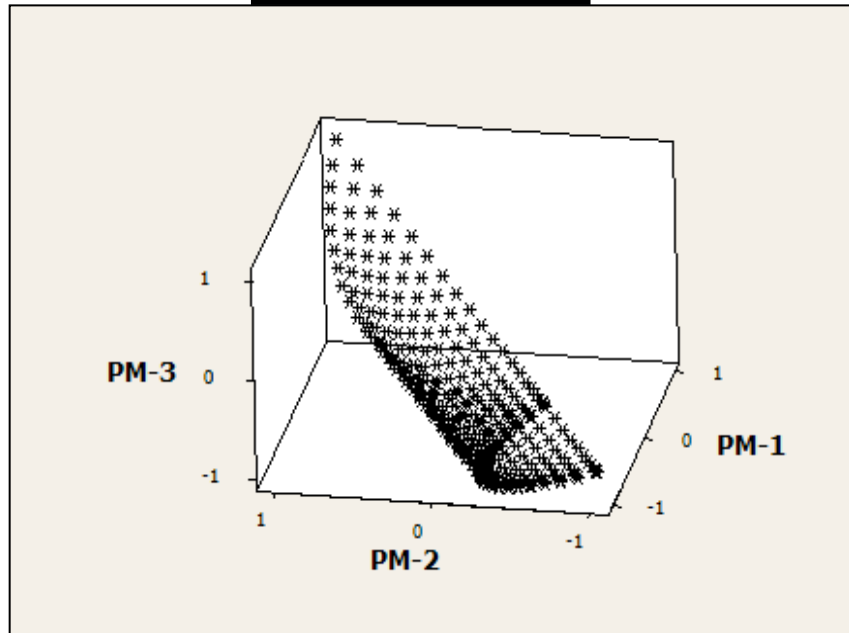
Feasible Region



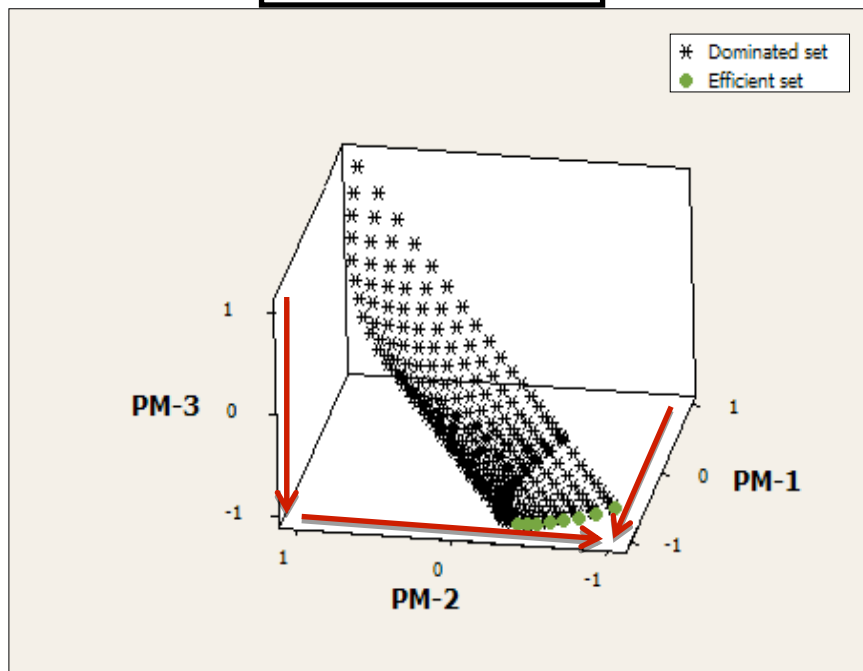
Efficient Frontier



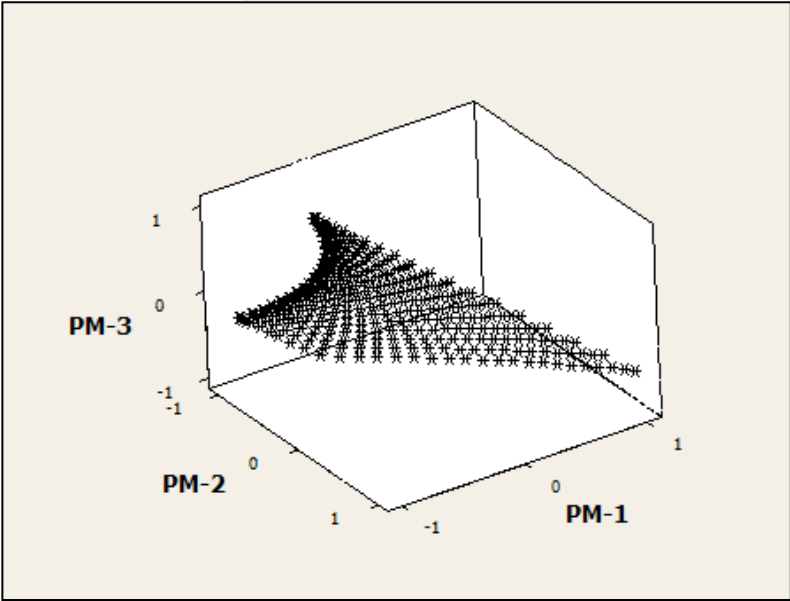
Feasible Region



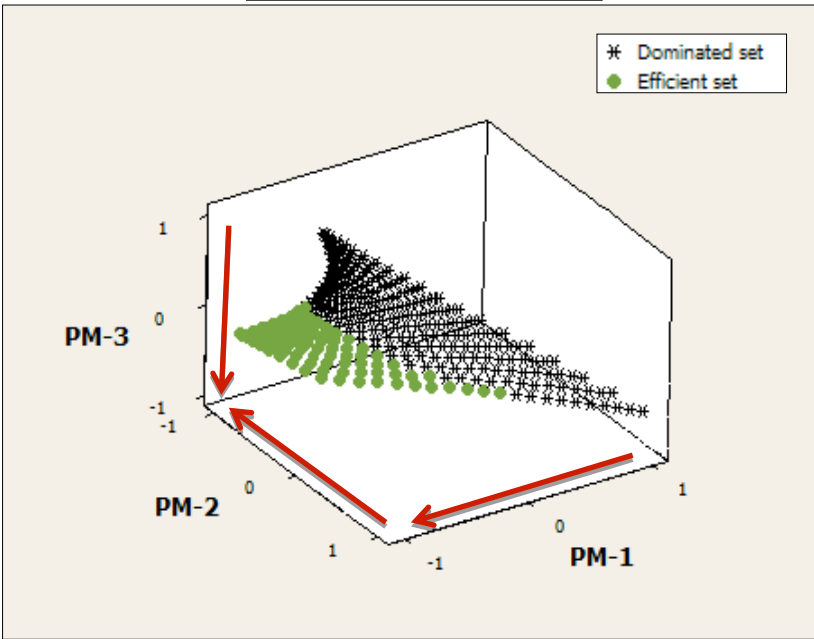
Efficient Frontier



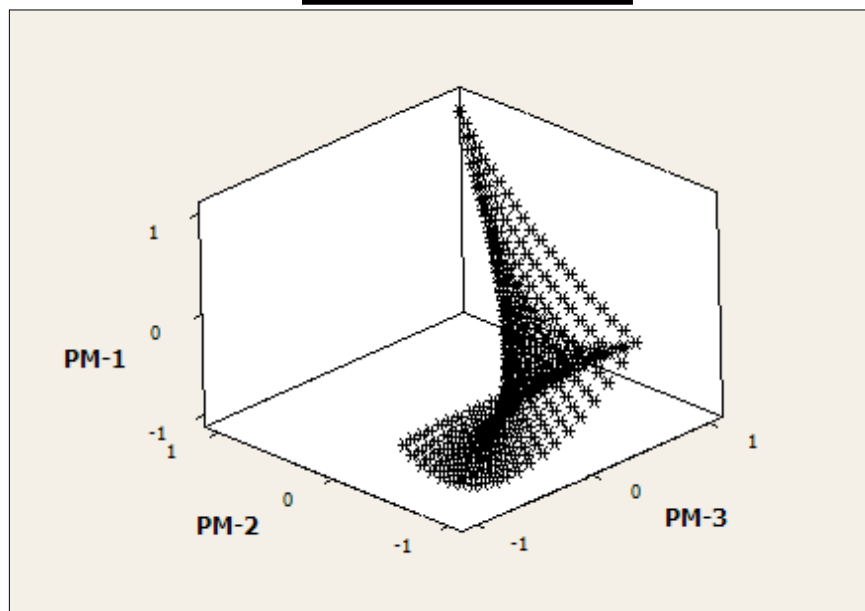
Feasible Region



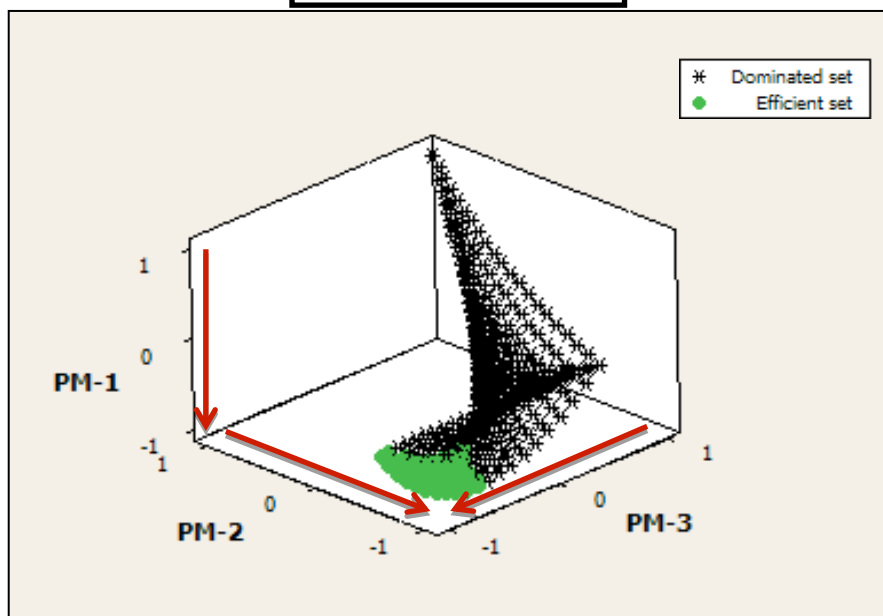
Efficient Frontier



Feasible Region



Efficient Frontier



11 APPENDIX D

This appendix shows the analysis of variance for case study 1.

Response Surface Regression: Total Weight versus Melt tempera, Packing pressure

Estimated Regression Coefficients for Total Weight (g)

Term	Coef	SE Coef	T	P
Constant	0.09993	0.01939	5.155	0.014
Melt temperature	-0.51900	0.01061	-48.912	0.000
Packing pressure	0.46431	0.01061	43.755	0.000
Melt temperature*Melt temperature	0.02030	0.01840	1.103	0.351
Packing pressure*Packing pressure	-0.08994	0.01838	-4.894	0.016
Melt temperature*Packing pressure	0.03197	0.01299	2.460	0.091

S = 0.0259914 PRESS = 0.0241289
R-Sq = 99.93% R-Sq(pred) = 99.18% R-Sq(adj) = 99.82%

Based on P-values, Total weight is significant affected by Melt temperature, Packing pressure and Packing pressure². The significant effect is selected based on the P-value < .05. The R-sq value is more than 99%.

Response Surface Regression: Volumetric S versus Melt tempera, Packing presure

Estimated Regression Coefficients for Volumetric Shrinkage (mm)

Term	Coef	SE Coef	T	P
Constant	-0.04368	0.017522	-2.493	0.088
Melt temperature	0.84304	0.009591	87.903	0.000
Packing pressure	-0.16997	0.009591	-17.721	0.000
Melt temperature*Melt temperature	0.03128	0.016629	1.881	0.157
Packing pressure*Packing pressure	0.05674	0.016611	3.416	0.042
Melt temperature*Packing pressure	0.04266	0.011744	3.632	0.036

S = 0.0234922 PRESS = 0.0198997
R-Sq = 99.96% R-Sq(pred) = 99.55% R-Sq(adj) = 99.90%

Based on P-values, Volumetric shrinkage is significant affected by Melt temperature, Packing pressure, Packing pressure² and the interaction between Melt temperature and Packing pressure. The R-sq value is more than 99%.

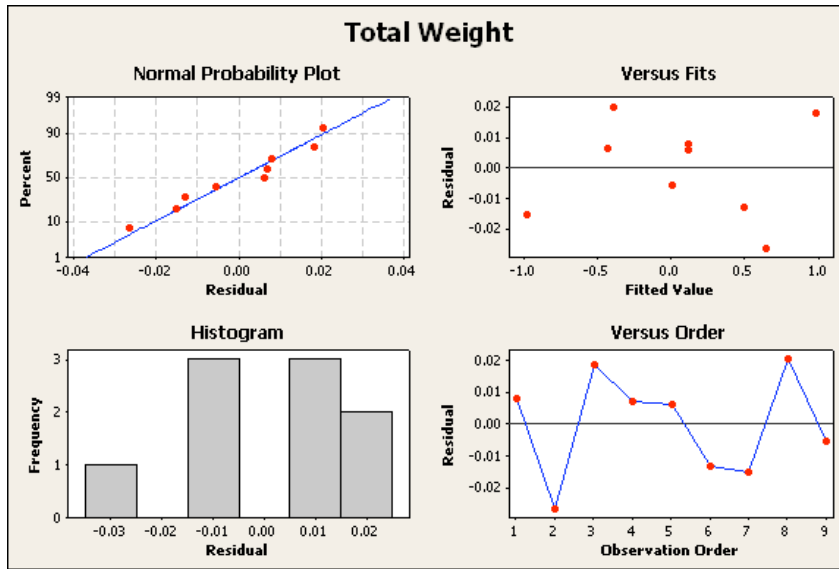


Figure 53. Residual plots of Total weight for case 1. The normal probability plot in the up left side shows that the points are adjusted at the line. The Residual versus fit plot in the up right side, shows that the points are randomly dispersed around the horizontal axis. In the down right side the residual versus order plot shows an independency between runs.

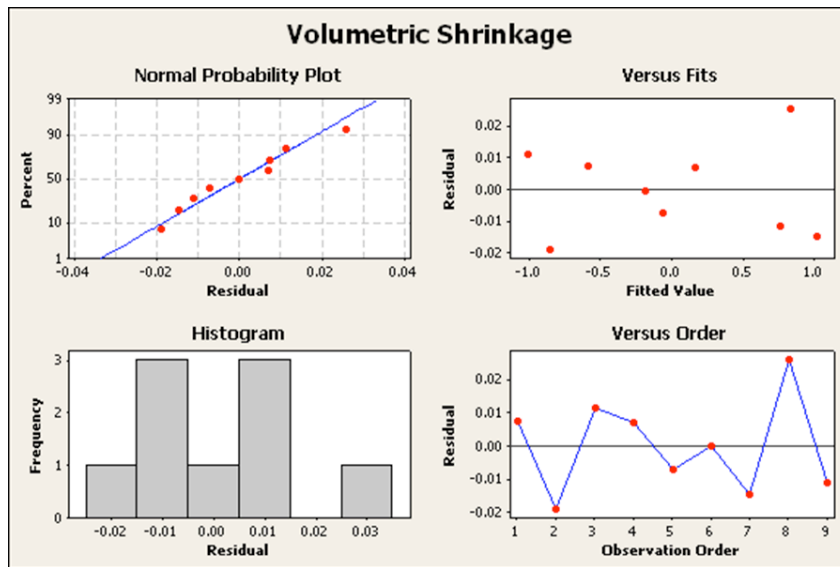


Figure 54. Residual plot of Volumetric shrinkage for case 1. The normal probability plot in the up left side shows that the points are adjusted at the line. The Residual versus fit plot in the up right side, shows that the points are randomly dispersed around the horizontal axis. In the down right side the residual versus order plot shows an independency between runs.

12 APPENDIX D

This appendix shows the analysis of variance for case study 2.

Response Surface Regression: Cycle Time (versus Melt Tempera, Mold Tempera

Estimated Regression Coefficients for Cycle Time (sec)

Term	Coef	SE Coef	T	P
Constant	-0.456286	0.004126	-110.595	0.000
Melt Temperature °C	0.041903	0.002260	18.543	0.000
Mold Temperature °C	0.961652	0.002260	425.556	0.000
Melt Temperature °C*	-0.003565	0.003914	-0.911	0.430
Melt Temperature °C				
Mold Temperature °C*	0.466544	0.003914	119.199	0.000
Mold Temperature °C				
Melt Temperature °C*	-0.006496	0.002768	-2.347	0.101
Mold Temperature °C				

S = 0.00553524 PRESS = 0.00111391
R-Sq = 100.00% R-Sq(pred) = 99.98% R-Sq(adj) = 100.00%

Based on P-values, Cycle time is significant affected by Melt temperature, Mold temperature and Mold temperature². The R-sq value is more than 99%.

Response Surface Regression: Total Weight versus Melt Tempera, Mold Tempera

Estimated Regression Coefficients for Total Weight (g)

Term	Coef	SE Coef	T	P
Constant	0.015716	0.004603	3.415	0.042
Melt Temperature °C	-0.928009	0.002521	-368.119	0.000
Mold Temperature °C	-0.074752	0.002521	-29.652	0.000
Melt Temperature °C*	-0.008281	0.004366	-1.897	0.154
Melt Temperature °C				
Mold Temperature °C*	-0.008682	0.004366	-1.988	0.141
Mold Temperature °C				
Melt Temperature °C*	0.002070	0.003088	0.671	0.551
Mold Temperature °C				

S = 0.00617504 PRESS = 0.00127854
R-Sq = 100.00% R-Sq(pred) = 99.98% R-Sq(adj) = 99.99%

Based on P-values, Total weight is significant affected by Melt temperature and Packing pressure. The R-sq value is more than 99%.

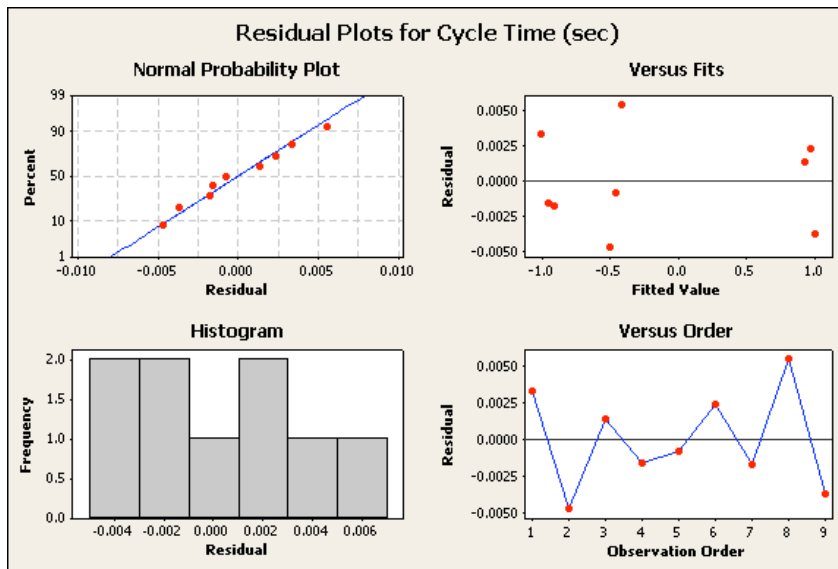


Figure 55. Residual plot for Cycle time. The normal probability plot in the up left side shows a good adjusted of the points considering the line. The Residual versus fit plot in the up right side, shows that the points are randomly dispersed around the horizontal axis. In the down right side the residual versus order plot shows an independency between runs around the horizontal axis.

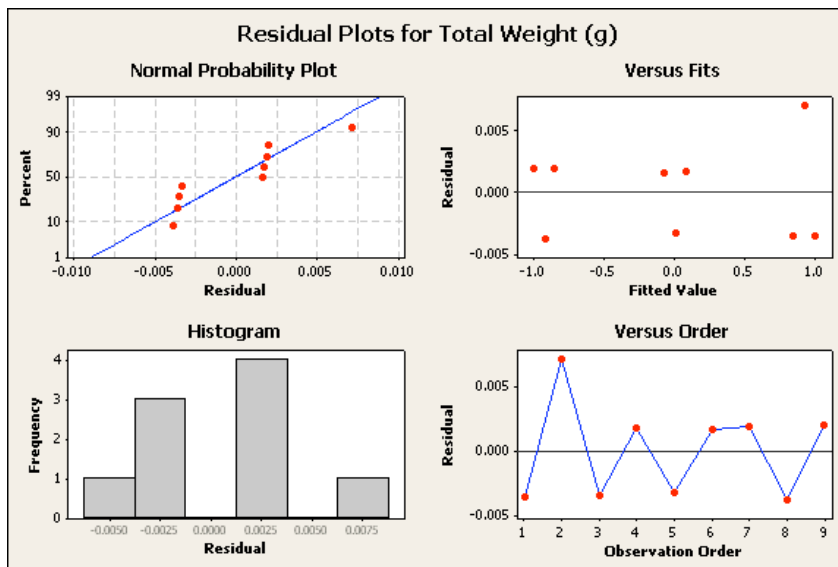


Figure 56. Residual plot for Total weight. The normal probability plot in the up left side shows that the points are adjusted at the line. The Residual versus fit plot in the up right side, shows that the points are randomly dispersed around the horizontal axis. In the down right side the residual versus order plot shows an independency between runs.

13 APPENDIX D

This appendix shows the analysis of variance for case study 3.

Response Surface Regression: Total Weight versus Melt tempera, Packing pressure

Estimated Regression Coefficients for Total Weight (g)

Term	Coef	SE Coef	T	P
Constant	0.11472	0.02426	4.728	0.018
Melt temperature	-0.51282	0.01328	-38.617	0.000
Packing pressure	0.46849	0.01328	35.276	0.000
Melt temperature*Melt temperature	0.01207	0.02303	0.524	0.636
Packing pressure*Packing pressure	-0.08432	0.02300	-3.666	0.035
Melt temperature*Packing pressure	0.04555	0.01626	2.801	0.068

S = 0.0325283 PRESS = 0.0367368
R-Sq = 99.89% R-Sq(pred) = 98.74% R-Sq(adj) = 99.71%

Based on P-values, Total weight is significant affected by Melt temperature, Packing pressure and Packing pressure². The R-sq value is more than 99%.

Response Surface Regression: Volumetric S versus Melt tempera, Packing pressure

Estimated Regression Coefficients for Volumetric Shrinkage (mm)

Term	Coef	SE Coef	T	P
Constant	-0.04745	0.06151	-0.771	0.497
Melt temperature	0.81764	0.03367	24.284	0.000
Packing pressure	-0.19111	0.03367	-5.676	0.011
Melt temperature*Melt temperature	0.05450	0.05838	0.933	0.419
Packing pressure*Packing pressure	0.01189	0.05832	0.204	0.852
Melt temperature*Packing pressure	0.02170	0.04123	0.526	0.635

S = 0.0824726 PRESS = 0.245544
R-Sq = 99.52% R-Sq(pred) = 94.24% R-Sq(adj) = 98.72%

Based on P-values, Volumetric shrinkage is significant affected by Melt temperature and Packing pressure. The R-sq value is more than 98%.

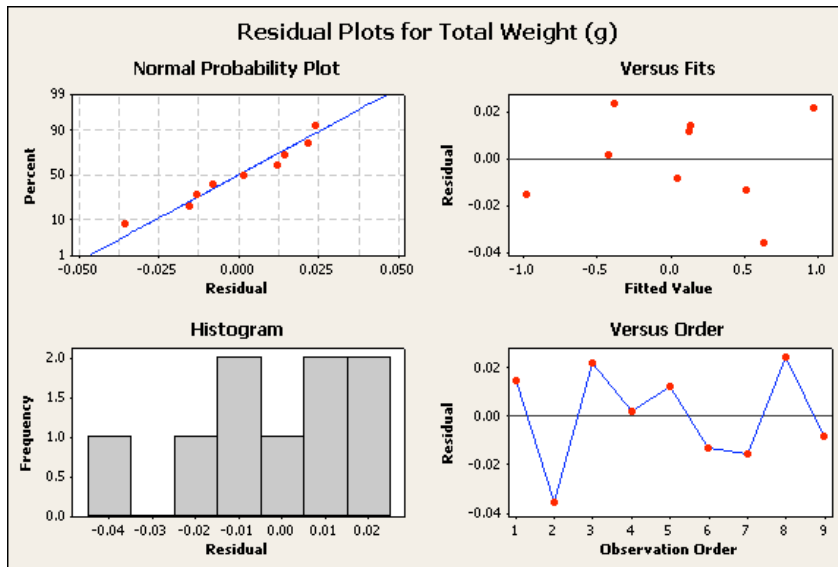


Figure 57. Residual plot for Total weight. The normal probability plot in the up left side shows that the points are adjusted at the line. The Residual versus fit plot in the up right side, shows that the points are randomly dispersed around the horizontal axis. In the down right side the residual versus order plot shows an independency between runs.

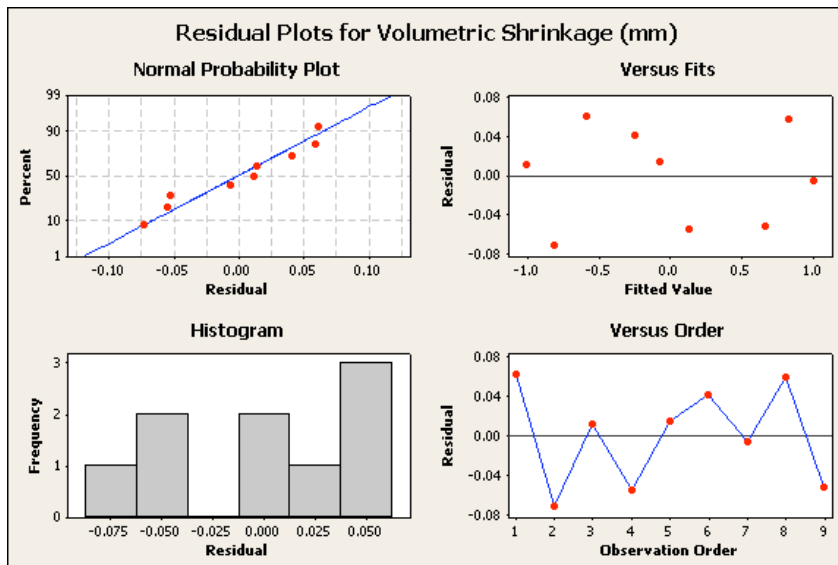


Figure 58. Residual plot for Volumetric shrinkage. The normal probability plot in the up left side shows that the points are adjusted at the line. The Residual versus fit plot in the up right side, shows that the points are randomly dispersed around the horizontal axis, and a not linear distribution, based on the test this data met the equal variance. In the down right side the residual versus order plot shows an independency between runs.